Gpyro – A Generalized Pyrolysis Model for Combustible Solids
Technical Reference

Version 0.800
May 1, 2014

Chris Lautenberger

Reax Engineering Inc.
1921 University Ave
Berkeley, CA 94704

510-629-4930 x801
lautenberger@reaxengineering.com

Acknowledgments

The financial support of NSF and NASA is gratefully acknowledged. Gpyro development was funded as part of NSF Award 0730556, "Tackling CFD Modeling of Flame Spread on Practical Solid Combustibles" (September 2007-September 2010). Development of early Gpyro versions was funded by the NASA Graduate Student Researcher Program under Grant #NNC-04HA08H, "Piloted Ignition and Flame Spread on Composite Materials in Partial and Normal Gravity" (August 2004 – August 2007).

Esther Kim at WPI and Amanda Dodd at UC Berkeley have played important roles in model development by serving as beta testers and exercising Gpyro in ways that were not contemplated during its initial development. I would like to thank them for their patience, their bug reports, and their suggestions as to how to improve Gpyro. Bryan Klein at NIST has helped get the source code and other files under Subversion control on Google Code. Thomas Steinhaus from the University of Edinburgh showed great patience as we worked together to get Gpyro running on a cluster there.

Contents

NOMENCLATURE

Letters

a	Coefficients in discretized equations or Thomas algorithm
A	Reactant species
A	Parameter in Equation 162
b	Coefficient in discretized equations or Thomas algorithm
b	Exponent in Equation 47
B	Product species or parameter in Equation 162
c	Specific heat capacity (J/kg–K)
c	Coefficient in Thomas algorithm
C	Parameter in Equation 162
d	Coefficient in Thomas algorithm or pore diameter (m)
D	Diffusivity (m^2/s) or parameter in Equation 162
D	Coefficient in discretized Equations, see e.g. Equation 127c
E	Activation energy (kJ/mole) or parameter in Equation 162
F	Coefficient in convective diffusive equations (Equation 145); parameter in Eq. 162
G	Parameter in Equation 162
h	Enthalpy (J/kg)
h_c	Convective heat transfer coefficient (W/m^2–K)
h_{cr}	Inverse contact resistance (W/m^2–K)
h_{cv}	Volumetric heat transfer coefficient (W/m^3–K)
ΔH	Change in enthalpy (J/kg)
$\dot{j}''_j$	Diffusive mass flux (kg/m^2–s)
J	Coefficient in convective–diffusive equation, see e.g. Equation 145
k	Thermal conductivity (W/m–K)
k_b	Boltzmann constant (J/K)
K	Permeability (m^2)
K	Number of condensed phase reactions
L	Number of homogeneous gas phase reactions or thickness (m)
m	Mass (kg)
m''	Mass per unit area (kg/m^2)
$\dot{m}''$	Mass flux (kg/m^2–s)
M	Number of condensed phase species
M	Molecular mass (g/mol or kg/mol)
n	Exponent (reaction order; Property exponent, Equation 4)
N	Number of gaseous species
p	Exponent in Equation 47
P	Pressure (Pa)
P	Cell Peclet number, e.g. Equation 127e
P	Coefficient in Thomas algorithm, Equation 130
Pr	Prandtl number
q	Exponent in Equation 47
$\dot{q}''$	Heat flux (W/m^2); $\dot{q}''$ is conductive, $\dot{q}''_r$ is radiative, $\dot{q}''_e$ is external radiative

Q	Coefficient in Thomas algorithm, Equation 130
$\dot{Q}'''$	Volumetric rate of heat release or absorption (W/m^3)
r	Reaction rate (kg/m^3–s)
R	Universal gas constant (J/mole–K)
s	Position of solidification front in Stefan problem (m)
S	Source term
Sc	Schmidt number
t	Time (s)
T	Temperature (K)
Δt	Time step (s)
X	Volume fraction (–)
y	Yield
Y	Mass fraction (–)
z	Distance (m)
Z	Condensed phase pre–exponential factor (s^{-1})
Z	Gas phase pre–exponential factor, Equation 47 (units of m, mole, K, s)
δz	Distance from center of grid one grid cell to center of adjacent grid cell (m)
Δz	Size (height) of grid cell (m)

Greek symbols

α	Relaxation parameter or conversion
β	Heating rate (K/min or K/s)
γ	Length scale (m) controlling radiant conductivity, see Equation 7
Γ	Effective diffusion coefficient in discretized equations
δ	Thickness (m)
ε	Emissivity (–)
ε	Energy of attraction between two molecules, Equation 19 (J)
ε	Small value
κ	In–depth radiation absorption coefficient (m^{-1})
ν	Viscosity (m^2–s)
ρ	Density (kg/m^3)
σ	Stefan–Boltzmann constant ($W/m^2–K^4$)
σ	Collision diameter of molecular species, Equation 19 (Å)
σ_m^2	Parameter in Equation 9c (K^2)
ϕ	Generic variable
χ	Parameter controlling swelling, see Equation 23 and 24
ψ	Porosity (–)
Ω	Function of dimensionless temperature
$\dot{\omega}'''$	Volumetric reaction rate (kg/m^3–s)

Subscripts

A	Species A
b	Baseline or bottom (interface value)
B	Species B
B	Bottom (cell center value)
d	Destruction or datum
D	Diffusivity
e	East (interface value)
e	External (as in $\dot{q}''_e$)
exp	Experimental
E	East (cell center value)
f	Formation
g	Gaseous, gas phase, or gasification
i	Condensed phase species i
j	Gaseous species j
k	Heterogeneous reaction k
ℓ	Homogeneous gas phase reaction ℓ
m	Melting
mod	Model
nb	No blowing
O_2	Oxygen
P	Point P
r	Reference (as in T_r) or radiative (as in k_r)
s	Solid phase (really, condensed phase)
sol	Solid
t	Top (interface value)
T	Top (cell center value)
vol	Volatilization
w	West (interface value)
W	West (cell center value)
0	Initial (as in T_0)
∞	Ambient
δ	At $z = \delta$
Σ	Integrated (summation)

Superscripts

$+$	Positive part of source term
$-$	Negative part of source term
$\bar{(\,)}$	Weighted or averaged
$\circ$	Value at present time
∞	Ambient

1.0 INTRODUCTION

This document is the Technical Reference to Gpyro, a generalized pyrolysis model for combustible solids (see http://reaxengineering.com/trac/gpyro). General background information, a discussion of the model's capabilities, and instructions for setting up and running Gpyro simulations can be found in the Users Guide [1]. Additional technical details can be found in Reference [2]. Both the Users' Guide and Technical Reference will be continuously updated as Gpyro evolves.

Gpyro solves a generalized set of coupled equations, rather than separate model equations for different classes of materials. A particular material is simulated by specifying a set of model parameters (thermophysical properties, reaction mechanism, etc.), and a particular experimental configuration is simulated by specifying initial and boundary conditions. The flexibility to invoke or omit submodels for various transport phenomena is provided because there may be little consequence to omitting a particular phenomenon from a simulation other than reducing the computational expense and the number of adjustable parameters. Instead of hardcoding a certain level of complexity in Gpyro, the user determines how much complexity or detail to include in a simulation. For example, thermophysical properties may be temperature–dependent or invariant with temperature; decomposition mechanisms can be single–step or multi–step; thermal radiation can be absorbed only at the surface or in–depth, and so on. Some of the physics embedded in the governing equations may be superfluous for practical engineering applications so they can be omitted from a simulation if desired.

At the heart of Gpyro, separate conservation equations are solved for gaseous and condensed phase mass, species, and energy as well as gas phase momentum using a Darcy's law approximation (Stokes flow). An arbitrary number of gas phase and condensed phase species can be accommodated, each having its own thermophysical properties. The user may specify any number of heterogeneous (solid/gas) or homogeneous (gas/gas) reactions. Both in–depth radiation absorption in a semi–transparent medium and radiation transport across pores are considered. Melting is modeled using a localized increase (Gaussian peak) in the apparent specific heat capacity. All volatiles generated inside the solid escape to the ambient with no resistance to flow unless the pressure solver is invoked to solve for the pressure distribution in the solid, in which case the resultant flow of volatiles is calculated according to Darcy's law. Similarly, the user may invoke a gas phase convective–diffusive solver that determines the composition of the volatiles, including diffusion of gaseous species from the ambient into the decomposing porous solid. Thus, in addition to calculating the mass flux of volatiles escaping from the solid, the actual composition of these vapors is calculated.

2.0 PRELIMINARIES, PROPERTIES, AND DEFINITIONS

Consider a condensed phase combustible material. It may contain as many as M chemically distinct condensed phase species. Examples of different condensed phase species include pure polymer, glass fiber reinforcements, char, and ash. Within a material, the initial concentrations of each species may be uniform (as in the case of a homogeneous blended composite) or vary spatially (as in the case of laminated composites). As the solid is heated, it may degrade to form N chemically distinct gaseous species. These species include hydrocarbon fragments, water vapor, carbon monoxide, etc. Furthermore, gaseous species may be consumed or produced by both heterogeneous (solid/gas) reactions and homogeneous (gas/gas) reactions

In this Technical Reference, the index i is used to denote condensed phase species and the index j is used to denote gaseous species. Thus, Y_i is the mass of condensed phase species i divided by the total mass of all condensed phase species, and Y_j is the mass of gaseous species j divided by the mass of all gaseous species. Note that Y_j is *not* the mass of gaseous species j divided by the mass of all gaseous and condensed phase species. As implied earlier, M is the number of condensed phase species and N is the number of gaseous species.

Thermophysical properties (k, ρ, and c) of each condensed-phase species are assumed to vary with temperature as $\phi(T) = \phi_0 (T / T_r)^{n_\phi}$, where ϕ_0 and n_ϕ are user-specified parameters and T_r is a user-specified reference temperature. Thus, Gpyro can accommodate general trends such as an increase in c with temperature. However, detailed temperature dependencies of the underlying thermophysical properties cannot be included. This is not necessarily a drawback because rarely are accurate temperature–dependent measurements of $k(T)$, $c(T)$, or $\rho(T)$ available, particularly at temperatures above 300 ºC that are relevant to burning. Additionally, few detailed property measurements are available for intermediate species such as char or ash. It was felt that the simplicity of a two–parameter approximation for thermophysical properties outweighs any potential drawbacks associated with the inability to specify detailed temperature dependent properties.

2.1 Bulk density and porosity

Since the condensed phase is composed of M distinct species, each having its own thermophysical properties, the effective properties appearing in the conservation equations presented later must be calculated from an appropriately weighted local composition. Some quantities are weighted by the local volume fraction, and others are weighted by the local mass fraction. The relation between mass fraction and volume fraction is:

$$X_i = \overline{\rho} \frac{Y_i}{\rho_i} \tag{1}$$

Here $\overline{\rho}$ is the weighted bulk density, ρ_i is the bulk density of condensed phase species i, X_i is the volume fraction of condensed phase species i, and Y_i is the mass fraction of condensed phase species i. An overbar denotes an averaged quantity, i.e. the weighted bulk density is:

$$\overline{\rho} = \sum_{i=1}^{M} X_i \rho_i \tag{2}$$

Weighted bulk density can also be calculated from condensed-phase species mass fractions:

$$\overline{\rho} = \left(\sum_{i=1}^{M} \frac{Y_i}{\rho_i} \right)^{-1} \tag{3}$$

The bulk density of each condensed phase species is assumed to vary with temperature according to the relation:

$$\rho_i(T) = \rho_{0,i} \left(\frac{T}{T_r} \right)^{n_{\rho,i}} \tag{4}$$

where $\rho_{0,i}$ and $n_{\rho,i}$ are user–specified parameters and T_r is a user–specified reference temperature, often (but not necessarily) taken as close to room temperature for convenience.

Note that in Equations 1 to 4, ρ_i is the bulk density of species *i* (in a vacuum if it is porous). Bulk density is defined as total mass divided by total volume, not the density of a pure nonporous solid. The designation of the bulk density of species *i* as ρ_i is different from nomenclature often used in other pyrolysis models where ρ_i is the mass of species *i* per unit volume of mixture (which would instead be represented here as $\overline{\rho} Y_i$).

To simplify Gpyro, it is assumed that porosity (ψ) is a "property" of each condensed phase species. This eliminates the need to solve a separate equation for porosity evolution because the weighted porosity can be calculated from the local composition as:

$$\overline{\psi} = \sum X_i \psi_i \tag{5}$$

The porosity of species *i*, denoted ψ_i, is calculated as follows:

$$\psi_i(T) = 1 - \frac{\rho_i(T)}{\rho_{s0,i}} \tag{6}$$

Where ρ_s denotes the "solid" density, i.e. the density of a pure nonporous solid, and $\rho_{s0,i}$ is a user–specified constant corresponding to the solid density of species *i* at a particular temperature. The quantity $\rho_i(T)$ is the bulk density of species *i* (Equation 4). The temperature-dependent porosity of species *i* is fixed via specification of $\rho_{0,i}$, $n_{\rho,,i}$, T_r, and $\rho_{s0,i}$. The small density contribution from the gases that fill the voids ($\overline{\psi}\rho_g$) does not affect Equation 4 because, as indicated earlier, the bulk density is formally defined under vacuum. This is more of a technical

than a practical consideration because $\overline{\psi}\rho_g << \overline{\rho}$ except under special circumstances. The quantity $\overline{\psi}\rho_g$ is calculated via the gas phase mass conservation equation, as described later.

2.2 Effective thermal conductivity

The effective thermal conductivity of a solid material is affected by its density, porosity, moisture content, microstructure, and orientation of wood grain or reinforcements. However, as with the presumed temperature dependency of condensed phase bulk density, a simple functional form for condensed–phase effective thermal conductivity is assumed:

$$k_i(T) = k_{s,i}(T) + k_{r,i}(T) = k_{0,i}\left(\frac{T}{T_r}\right)^{n_{k,i}} + \gamma_i \sigma T^3 \tag{7}$$

As with bulk density and porosity, the averaged effective thermal conductivity is weighted by condensed phase volume fractions:

$$\overline{k} = \sum_{i=1}^{M} X_i k_i \tag{8}$$

In Equation 7, the effective thermal conductivity of each condensed phase species is broken into a solid and a radiative component ($k_{s,i}$ and $k_{r,i}$ respectively). The latter is attributed to radiation heat transfer across pores and may become a dominant mode of heat transfer in porous media at high temperatures. The parameter γ_i controls the radiative contribution to the effective thermal conductivity. It has units of length and depends on the pore structure and other considerations (see Ref. [2] for details). Radiative transport across pores can be omitted by setting $\gamma_i = 0$.

It is inherently assumed that the effective thermal conductivity specified by setting $k_{0,i}$, $n_{k,i}$, and γ_i in Equation 7 takes into account bulk density, porosity, etc. This is commensurate with the spirit of the present work, which aims to formulate a generalized model and code the governing equations in a self–consistent manner rather than consider detailed submodels for thermophysical properties of specific materials. There are several models in the literature that can be used to estimate effective thermal conductivities on the basis of bulk density, porosity, grain orientation, etc. The user is free to use such models as the basis for specifying $k_{0,i}$ $n_{k,i}$ and γ_i in Equation 7.

2.3 Apparent specific heat capacity

The temperature–dependent specific heat capacity of species i is assumed to be the sum of a "baseline" specific heat ($c_{b,i}$) and (for polymers that melt) the apparent increase in the specific heat capacity due to the latent heat of melting ($c_{m,i}$):

$$c_i(T) = c_{b,i}(T) + c_{m,i}(T) \tag{9a}$$

$$c_{b,i}(T) = c_{0,i}\left(\frac{T}{T_r}\right)^{n_{c,i}} \tag{9b}$$

The latent heat of melting (ΔH_m) is assumed to be distributed via a Gaussian peak centered at T_m, the melting temperature:

$$c_{m,i}(T) = \frac{\Delta H_{m,i}}{\sqrt{2\pi\sigma_{m,i}^2}}\exp\left(-\frac{(T-T_{m,i})^2}{2\sigma_{m,i}^2}\right) \tag{9c}$$

In Equation 9c, σ_m^2 is a model parameter having units of K^2 that controls the "width" of the Gaussian specific heat capacity peak attributed to the latent heat of melting. If a condensed phase species with constant specific heat capacity is desired, then the user sets $n_{c,i} = 0$ and $\Delta H_{m,i} = 0$. Inherent in Equation 9c is the assumption that a condensed phase species melts over a range of temperatures rather than at a single temperature. This is not necessarily a shortcoming because only crystalline solids have a well–defined melting temperature. Most polymers are a mixture of crystalline and amorphous components so that melting (or softening of the amorphous components) usually occurs over a finite temperature range.

The sensible enthalpy of condensed phase species i at temperature T is determined by integration of Equation 9a after substituting Equations 9b and 9c. The result is:

$$\begin{aligned} h_i(T) &= \int_{T_d}^{T}\left(c_{b,i}(\theta)+c_{m,i}(\theta)\right)\mathrm{d}\theta \\ &= \frac{c_{0,i}}{n_{c,i}+1}\left(T\left(\frac{T}{T_r}\right)^{n_{c,i}} - T_d\left(\frac{T_d}{T_r}\right)^{n_{c,i}}\right) + \frac{\Delta H_{m,i}}{2}\left(\mathrm{erf}\left(\frac{T-T_{m,i}}{\sqrt{2\sigma_{m,i}^2}}\right) - \mathrm{erf}\left(\frac{T_d-T_{m,i}}{\sqrt{2\sigma_{m,i}^2}}\right)\right) \end{aligned} \tag{10}$$

Note that T_d is the temperature datum used to establish an absolute value of enthalpy (it is not necessarily the same as the ambient, initial, or reference temperature). In Gpyro, the temperature datum is arbitrarily taken as 200 K.

Enthalpy and specific heat capacity are weighted by mass fractions:

$$\overline{c} = \sum_{i=1}^{M} Y_i c_i \tag{11}$$

$$\overline{h} = \sum_{i=1}^{M} Y_i h_i \tag{12}$$

2.4 Radiative properties

The user must also specify for each condensed-phase species an emissivity (ε_i, dimensionless) and radiative absorption coefficient (κ_i, m^{-1}). Emissivity controls the fraction of the incident radiation absorbed at the surface and the fraction of the blackbody emissive power of the surface that is radiated away. The radiative absorption coefficient controls the depth over which incident thermal radiation is attenuated, see Equations 66 and 67. Radiative properties are weighted by volume:

$$\bar{\varepsilon} = \sum_{i=1}^{M} X_i \varepsilon_i \tag{13}$$

$$\bar{\kappa} = \sum_{i=1}^{M} X_i \kappa_i \tag{14}$$

2.5 Permeability

If the pressure solver is invoked, each condensed phase species must be assigned a permeability. The weighted permeability is calculated on a volume basis:

$$\overline{K} = \sum_{i=1}^{M} X_i K_i \tag{15}$$

2.6 Gas density and molecular weight

In addition to condensed-phase properties, specification of several gas-phase properties is required. The gas-phase density is calculated from the ideal gas law:

$$\rho_g = \frac{P\overline{M}}{RT_g} \tag{16}$$

In Equation 16, R is the universal gas constant , and $\overline{M}$ is calculated from the local volume fractions of all gaseous species:

$$\overline{M} = \sum_{j=1}^{N} X_j M_j \tag{17}$$

2.7 Gaseous specific heat capacity and enthalpy

It is assumed that all gaseous species have equal specific heat capacities that are independent of temperature. This approximation is justified given that little is known about the actual composition of the gaseous volatiles produced during the pyrolysis and gasification of practical materials. As with the condensed phase enthalpy, the gas phase sensible enthalpy is weighted by mass:

$$\bar{h}_g = \sum_{j=1}^{N} Y_j h_{g,j} = c_{pg}\left(T_g - T_d\right) \tag{18}$$

where c_{pg} denotes the (constant) gaseous specific heat capacity.

2.8 Gaseous mass diffusivity, thermal conductivity, and viscosity

Gaseous diffusion coefficients are calculated from Chapman–Enskog theory. The binary diffusion coefficient (units of m^2/s) for species A diffusing into species B is:

$$D_{AB} = 0.018829 \frac{\sqrt{T^3\left(\frac{1}{M_A} + \frac{1}{M_B}\right)}}{P\sigma_{AB}^2 \Omega_{D,AB}} \tag{19a}$$

In Equation 19a, M_A and M_B have units of g/mol, σ_{AB} is a weighted collision diameter of species A and B (units of Å), k_b is the Boltzmann constant, and ε_{AB} is the maximum energy of attraction between molecules A and B. Thus, σ_{AB} and $(\varepsilon/k_b)_{AB}$ are model parameters that describe the binary diffusion coefficient of species A into species B. These parameters are tabulated for several gases by Bird *et al.* [7], along with $\Omega_{D,AB}$ as a function of $T/\left(\varepsilon_{AB}/k_b\right)$. Note that σ_{AB} and ε_{AB} are weighted averages between molecules A and B:

$$\sigma_{AB} = \frac{1}{2}\left(\sigma_A + \sigma_B\right) \tag{19b}$$

$$\varepsilon_{AB} = \sqrt{\varepsilon_A \varepsilon_B} \tag{19c}$$

Since little is known about the composition of gaseous volatiles for practical materials, several approximations are made to simplify the gas phase calculations. It is assumed that all gaseous species have the same diffusivity ($D_{AB} = D$), taken as that of oxygen into the (user-specified) background species. Unit Prandtl, Schmidt, and Lewis numbers are (Pr = Sc = 1). It follows from these approximations:

$$k_g \approx \rho_g D c_{pg} \tag{20a}$$

$$\nu \approx D \tag{20b}$$

Equation 20a allows for considerable simplification of the gas phase energy equation.

To summarize, in addition to molecular weight, there are five gas phase properties: k_g, ρ_g, D, c_{pg}, and ν. ρ_g is calculated from Equation 16, c_{pg} is a user–specified constant, D is calculated from Equation 19, and the remaining two properties (k_g and ν) are calculated from the relations in Equation 20.

3.0 REACTION RATES AND SOURCE TERMS

The governing equations, presented in the next chapter, contain source terms attributed to reactions that must be quantified. In Gpyro, two types of reactions are considered: heterogeneous (solid/gas) and homogeneous (gas-gas).

Heterogeneous reactions involve the destruction of a condensed phase species to form gases and/or additional condensed phase species. An example is char formation wherein one condensed phase species (e.g., wood) is converted to a second condensed phase species (e.g., char) with the release of gases (pyrolysate). Some heterogeneous reactions may also involve the consumption of gases. For example, in heterogeneous char oxidation, oxygen is consumed and partially oxidized gaseous species are produced. Catalytic reactions are a special case of heterogeneous reactions and can be simulated with Gpyro. Solid–solid phase change or glass transition could be modeled as solid-phase reactions with Gpyro; technically these would be homogeneous solid-solid processes, but in the discussion that follows they would be considered heterogeneous reactions.

Homogeneous gas phase reactions involve only gases and do not involve the condensed phase. Examples of such reactions include tar cracking (where large tar molecules are broken into smaller hydrocarbon molecules) and the oxidation of gaseous pyrolysate.

3.1 Heterogeneous reaction stoichiometry

A particular condensed phase reaction is denoted by the index k, and the total number of condensed phase reactions is designated K (not to be confused with permeability; it should be clear from context which is meant). In the combustion literature, stoichiometry of gas phase reactions is often expressed using molar "ν" coefficients; the same is done here, with the important difference that the ν coefficients are given on a mass basis. Heterogeneous reactions are represented in Gpyro as:

$$1\,\text{kg } A_k + \sum_{j=1}^{N} \nu'_{j,k}\ \text{kg gas } j \rightarrow \nu_{B,k}\ \text{kg } B_k + \sum_{j=1}^{N} \nu''_{j,k}\ \text{kg gas } j \tag{21a}$$

$$\nu_{B,k} = \text{SF}_k \tag{21b}$$

$$\nu'_{j,k} = -\left(1-\text{SF}_k\right)\min\left(y_{s,j,k},0\right) \tag{21c}$$

$$\nu''_{j,k} = \left(1-\text{SF}_k\right)\max\left(y_{s,j,k},0\right) \tag{21d}$$

A_k denotes the condensed phase reactant species (the condensed phase species consumed by reaction k) and B_k denotes the condensed phase product species (the condensed phase species generated by reaction k). The composition of the gases consumed and produced by a heterogeneous reaction is controlled by the parameters $\nu'_{j,k}$ and $\nu''_{j,k}$. In Equation 21a, $\nu'_{j,k}$ is the

net mass of gaseous species j consumed by reaction k, and $\nu''_{j,k}$ is the net mass of gaseous species j produced by reaction k per unit mass of A_k consumed.

In order to generalize and simplify the specification of $\nu'_{j,k}$ and $\nu''_{j,k}$, a user–defined "species yield matrix" is introduced. This N by K matrix (recall that N is the total number of gaseous species and K is the number of heterogeneous reactions) is denoted $y_{s,j,k}$ and appears on the RHS of Equations 21c and 21d. The entries of $y_{s,j,k}$ may be positive or negative, with a positive entry corresponding to net production of a gaseous species by a particular reaction, and a negative entry corresponding to net consumption of a gaseous species by a particular reaction. The physical meaning of each entry in the species yield matrix is the net mass of gas phase species j consumed or generated by reaction k per unit mass of condensed phase that is converted to gases by reaction k. The sum of all entries in any column of the species yield matrix must add to 1 to conserve mass, and this must be strictly adhered to or nonphysical results will occur. Substitution of Equations 21b, 21c, and 21d into Equation 21a results in a balanced equation (conserves mass) only if $\sum_{j=1}^{N} y_{s,j,k} = 1$.

The ν coefficients are related to the "solid fraction" (SF) of reaction k, denoted SF_k, see Equation 21b - 21d. The solid fraction of reaction k is the fraction of condensed phase species A_k's mass that is converted to condensed phase species B_k. Extending this terminology, $1 - \mathrm{SF}_k$ could be called the "gas fraction" of reaction k. The solid fraction is related to the bulk densities of condensed phase reactant and product species A_k and B_k as:

$$\mathrm{SF}_k = 1 + \left(\frac{\rho_{B_k}}{\rho_{A_k}} - 1 \right) \chi_k \tag{22}$$

Since bulk densities may depend on temperature, SF_k may be a function of temperature. In Equation 22, the parameter χ_k is the fraction of the bulk density difference between condensed phase species A_k and B_k that is converted to gases. This is discussed in Section 3.3.

Gpyro assumes that each condensed phase reaction k consumes a single condensed phase species (A_k) and forms a single condensed phase species (B_k) plus gases. Although each condensed phase reaction k transforms a single condensed phase species (A_k) into at most one additional condensed phase species (B_k) plus gases, the user may specify multiple reactions that transform condensed phase species A to different species. Consequently, reactions of the type $A \rightarrow B + C$ can be accommodated with Gpyro via specification of multiple reactions that transform reactant A into different products.

A pyrolysis mechanism in the form of Equation 21a can be converted to the present treatment using the relations in Equations 21 and 22.

3.2 Heterogeneous reactions - volumetric source terms

In Section 3.3 below, kinetics considerations are used to develop an expression for $\dot{\omega}'''_{dA_k}$, the local volumetric destruction rate of condensed-phase reactant A_k. In Gpyro, local volumetric formation or destruction rates of all other condensed/gaseous species by heterogeneous reactions are related to $\dot{\omega}'''_{dA_k}$ via the stoichiometry presented in Section 3.1. Volumetric source terms are needed because the conservation equations presented later contain volumetric reaction rates.

The formation rate of condensed phase species B_k by reaction k ($\dot{\omega}'''_{fB_k}$) and the rate at which the mass of condensed phase species A_k is volatilized or converted to gases by reaction k ($\dot{\omega}'''_{fg_k}$) are calculated, respectively, from Equations 23 and 24:

$$\dot{\omega}'''_{fB_k} = \mathrm{SF}_k \dot{\omega}'''_{dA_k} = \left(1 + \left(\frac{\rho_{B_k}}{\rho_{A_k}} - 1\right)\chi_k\right)\dot{\omega}'''_{dA_k} \tag{23}$$

$$\dot{\omega}'''_{fg_k} = (1 - \mathrm{SF}_k)\dot{\omega}'''_{dA_k} = \left(1 - \frac{\rho_{B_k}}{\rho_{A_k}}\right)\chi_k \dot{\omega}'''_{dA_k} \tag{24}$$

The solid fraction of reaction k (SF_k) that appears in Equations 23 and 24 is defined in Equation 22. Recall that SF is the fraction of the mass of condensed phase species A that is converted to condensed phase species B; the remainder of the mass of condensed phase species A is volatilized, i.e. converted to gases (Equation 24). Adding Equations 23 and 24 gives:

$$\dot{\omega}'''_{fB_k} + \dot{\omega}'''_{fg_k} = \dot{\omega}'''_{dA_k} \tag{25}$$

Equation 25 says that for reaction k, the rate at which condensed phase species A_k is converted to condensed phase species B_k plus the rate at which condensed phase species A_k is converted to gases equals the destruction rate of condensed phase species A_k.

Equation 24 above gives the formation rate of all gases by reaction k ($\dot{\omega}'''_{fg_k}$). However, it does not provide any information about the production/destruction rates of individual gaseous species (or equivalently, the composition of the gases that are generated or consumed by that reaction). This information is provided via the user–specified species yield matrix $y_{s,j,k}$ mentioned earlier. Specifically, the formation and destruction rates of gaseous species j from condensed phase reaction k are calculated as:

$$\dot{\omega}'''_{s,fj,k} = \dot{\omega}'''_{fg_k} \max\left(y_{s,j,k}, 0\right) \tag{26}$$

$$\dot{\omega}'''_{s,dj,k} = -\dot{\omega}'''_{fg_k} \min\left(y_{s,j,k}, 0\right) \tag{27}$$

where $y_{s,j,k}$ is the N by K species yield matrix. See the text following Equation 21 for additional discussion about $y_{s,j,k}$. The subscript s stands for "solid" as a reminder that gaseous species may also be formed or destroyed by homogeneous gas phase reactions (discussed later).

Note that $\dot{\omega}'''_{fg_k}$ is the rate at which the mass of condensed phase species A_k is volatilized (converted to gases) by reaction k. It is not necessarily the same as the total production rate of gases as illustrated by the following example: Consider a char oxidation reaction where gaseous oxygen is consumed at a rate of 2 kg/m^3–s and solid char is consumed at a rate of 1 kg/m^3–s to produce 3 kg/m^3–s of product gases. In this case, $\dot{\omega}'''_{fg_k}$ would be 1 kg/m^3–s (not 3 kg/m^3–s) because although a total of 3 kg/m^3–s of product gases are being produced, only 1 kg/m^3–s of this originated in the condensed phase as the mass of species A_k.

The volumetric source terms above apply to a single reaction k. However, the conservation equations contain total source terms, which are obtained by summing over all reactions. The total destruction and formation rates of gases due to heterogeneous reactions are calculated by summing over Equations 26 and 27:

$$\dot{\omega}'''_{s,dj} = \sum_{k=1}^{K} \dot{\omega}'''_{s,dj,k} \tag{28}$$

$$\dot{\omega}'''_{s,fj} = \sum_{k=1}^{K} \dot{\omega}'''_{s,fj,k} \tag{29}$$

The total formation rate of all gases by volatilization of the condensed phase ($\dot{\omega}'''_{fg}$) is calculated by summing Equation 24 over all condensed phase reactions:

$$\dot{\omega}'''_{fg} = \sum_{k=1}^{K} \dot{\omega}'''_{fg_k} \tag{30}$$

The total destruction rate of condensed phase species i, and the total formation rate of condensed-phase species i, are calculated as:

$$\dot{\omega}'''_{di} = \sum_{k=1}^{K} \delta_{i,A_k} \dot{\omega}'''_{dA_k} \tag{31}$$

$$\dot{\omega}'''_{fi} = \sum_{k=1}^{K} \delta_{i,B_k} \dot{\omega}'''_{fB_k} \tag{32}$$

In Equations 31 and 32, δ is the Kronecker delta, which has the properties for general indices i and j:

$$\delta_{i,j} = \begin{cases} 1 & \text{if } i = j \\ 0 & \text{if } i \neq j \end{cases} \tag{33}$$

In Equation 33, i and j don't represent condensed and gaseous species as elsewhere.

3.3 Heterogeneous reactions - noncharring, charring, and intumescent

A noncharring reaction forms no condensed phase residue, and condensed phase reactant species A_k is transformed completely to product gases. This type of reaction is invoked in Gpyro by setting $\chi_k = 1$ and specifying no condensed-phase product species B_k. It can be seen from Equation 23 that SF_k becomes zero if $\rho_{B_k} = 0$ and $\chi_k = 1$. Consequently, the formation rate of condensed phase species B_k is also zero. At the same time, the quantity 1 – SF_k in Equation 24 (one minus the solid fraction) becomes 1, meaning that only gases are generated. Mass conservation requires that this type of reaction causes surface regression. Note that χ_k must be set equal to 1 for a noncharring reaction or mass will not be conserved.

For charring and intumescent reactions, the degree of shrinkage or swelling is controlled by the parameters χ_k, ρ_{A_k}, and ρ_{B_k}. As will be described below, these parameters can be used to simulate charring reactions that result in no net volume change, charring reactions where swelling occurs (intumescence), charring reactions where shrinkage occurs, and condensation reactions where gas-phase mass is converted to condensed-phase mass.

If $\chi_k = 1$ and $0 < \rho_{B_k} < \rho_{A_k}$, a charring reaction with no volume change will occur. It can be seen from Equations 23 and 24 that, in this case, the formation rate of condensed phase species *B* and gases are both nonzero. This is similar to the traditional approach to modeling the pyrolysis of charring materials.

Equations 23 and 24 can also be used to model an intumescent reaction with swelling by setting $0 \le \chi_k < 1$. Then, provided $\rho_{B_k} < \rho_{A_k}$, a lower density solid is formed from a higher density solid and swelling occurs to conserve mass. Essentially, the decrease in $\overline{\rho}$ is compensated for by an increase in the size of a grid cell through the condensed phase mass conservation equation, leading to swelling. In the extreme case of $\chi_k = 0$, swelling occurs without any escape of gases. Values of χ_k between 0 and 1 cause intumescence (swelling) to occur simultaneously with the release of gaseous vapors. The relative amounts of swelling and volatilization are dictated by the value of χ_k (closer to 0 means more swelling, and closer to 1 means more volatilization).

Values of χ_k between 1 and $\rho_{A,k}/\left(\rho_{A,k} - \rho_{B,k}\right)$ can be used to simulate a charring reaction that results in shrinkage (provided $\rho_{B_k} < \rho_{A_k}$). Essentially, the decreased formation rate of condensed phase species B_k (see Equation 23 and note that the term in parentheses is negative) caused by a value of χ_k greater than 1 leads to a decrease in the local grid size through the condensed phase mass conservation equation.

Finally, values of χ_k greater than $\rho_{A,k}/\left(\rho_{A,k} - \rho_{B,k}\right)$ can be used to simulate condensation reactions where gas phase mass is converted to condensed phase mass.

The preceding discussion assumes that $\rho_{B_k} < \rho_{A_k}$ and therefore a lower density solid is formed from a higher density (for example, char formed from wood has a lower density than the virgin wood). However, the case where $\rho_{B_k} > \rho_{A_k}$ is also conceivable, and the behavior is essentially the opposite of intumescence. If $\chi_k = 0$, then shrinkage would occur with no change in mass. This could be used to model a porous material that melts or collapses when heated. If $\chi_k = 1$, then no volume change would occur, but an increase in mass would occur (negative mass loss rate). For $0 < \chi_k < 1$, shrinkage would occur simultaneously with mass gain, with the relative amounts of shrinkage and mass gain dictated by the value of χ_k.

To summarize, a heterogeneous reaction causes shrinkage or swelling only when $\chi_k \neq 1$, with the noted exceptions that mass conservation requires noncharring reactions to cause surface regression and if $\rho_{B_k} > \rho_{A_k}$ then shrinkage and mass gain can occur depending on the value of χ_k (see preceding paragraph).

3.4 Heterogeneous reaction kinetics

Pyrolysis reaction stoichiometry and calculation of analogous volumetric source terms are described above, but the rate at which reactions occur (kinetics) must also be quantified. The starting point for the treatment of condensed phase decomposition kinetics is an equation often used to analyze TGA data with a single-step, n^{th} order reaction:

$$\frac{\mathrm{d}\alpha}{\mathrm{d}t} = Z \exp\left(-\frac{E}{RT}\right)(1-\alpha)^n \tag{34}$$

In Equation 34, α is the conversion (dimensionless), Z is the pre-exponential factor (s^{-1}), E is the activation energy (kJ/mol), and n is the reaction order. Note that the conversion is related to the instantaneous mass (m) and the initial mass (m_0) as $\alpha = 1 - m/m_0$. Since Equation 34 implies a single–step reaction, several changes are required before it can be generalized to accommodate multi–step reactions. Details are given in Ref. [2] and summarized below.

Define α_i as the conversion of condensed phase species i. This quantity is tracked locally in each cell, so $1 - \alpha_i$ can be calculated in a cell having size Δz as:

$$1 - \alpha_i = \frac{m_i''}{m_{i\Sigma}''} = \frac{\bar{\rho} Y_i \Delta z}{\left(\bar{\rho} Y_i \Delta z\right)_\Sigma} \tag{35}$$

In Equation 35, the numerator is the mass per unit area of condensed phase species i in a particular cell; the denominator is the initial (i.e., at $t = 0$) mass per unit area of condensed phase species i in that same cell plus the cumulative formation of species i through time t in that cell:

$$\left(\bar{\rho} Y_i \Delta z\right)_\Sigma \equiv \left(\bar{\rho} Y_i \Delta z\right)\Big|_{t=0} + \int_0^t \dot{\omega}_{fi}'''(\tau)\Delta z(\tau)\,\mathrm{d}\tau \tag{36}$$

The subscript Σ serves as a reminder that $\left(\bar{\rho} Y_i \Delta z\right)_\Sigma$ includes an integral (evaluated numerically as a summation). Note that $\dot{\omega}'''_{fi} \geq 0$ because $\dot{\omega}'''_{fi}$ is the formation rate of condensed phase species *i* (not the formation rate minus the destruction rate). Thus, the quantity $\left(\bar{\rho} Y_i \Delta z\right)_\Sigma$ remains constant or increases monotonically; it can never decrease. Since conversion (Equation 35) is tracked separately in each cell, from a kinetics standpoint each cell behaves as if it was a TGA sample.

After some manipulation [2] the destruction rate of species *i* by reaction *k* is calculated as:

$$\dot{\omega}'''_{di,k} = \left(1-\alpha_i\right)^{n_k} \frac{\left(\bar{\rho} Y_i \Delta z\right)_\Sigma}{\Delta z} Z_k \exp\left(-\frac{E_k}{RT}\right) \delta_{i,A_k} \tag{37}$$

The Kronecker delta is used to emphasize that for reaction *k* with A_k as the condensed-phase reactant species and stoichiometry given by Equation 21, species *i* is destroyed only if $i = A_k$. Thus, Equation 37 can be recast in terms of A_k:

$$\dot{\omega}'''_{dA_k,k} \equiv \dot{\omega}'''_{dA_k} = \left(1-\alpha_{A_k}\right)^{n_k} \frac{\left(\bar{\rho} Y_{A_k} \Delta z\right)_\Sigma}{\Delta z} Z_k \exp\left(-\frac{E_k}{RT}\right) \tag{38}$$

Equation 38 is used as the basis for the treatment of heterogeneous reaction source terms in Gpyro after making use of Equation 35 and including a multiplicative function $g\left(Y_{O_2}\right)$ to account for the effect of the presence of oxygen on the reaction rate. The final form of the heterogeneous reaction rate for a general n^{th} order reaction is:

$$r_k = \dot{\omega}'''_{dA_k} = f\left(\alpha_{A_k}\right) \frac{\left(\bar{\rho} Y_{A_k} \Delta z\right)_\Sigma}{\Delta z} Z_k \exp\left(-\frac{E_k}{RT}\right) g\left(Y_{O_2}\right) H\left(T - T_{crit,k}\right) \tag{39a}$$

$$f\left(\alpha_{A_k}\right) = \left(1-\alpha_{A_k}\right)^{n_k} = \left(\frac{\bar{\rho} Y_{A_k} \Delta z}{\left(\bar{\rho} Y_{A_k} \Delta z\right)_\Sigma}\right)^{n_k} \tag{39b}$$

Here, $f\left(\alpha_{A_k}\right)$ is the reaction model, assumed to be n^{th} order by default per Equation 39b (alternate reaction models are discussed in Section 3.4.1). $H\left(T - T_{crit,k}\right)$ is the Heaviside step function (equal to 0 for $T - T_{crit,k} < 0$, and equal to 1 for $T - T_{crit,k} \geq 0$). This effectively forces the reaction rate to be zero below $T_{crit,k}$. The k^{th} reaction rate (r_k) is the destruction rate of condensed phase species A_k by condensed phase reaction *k* and is denoted $\dot{\omega}'''_{dA_k}$. For each reaction *k*, the index of the condensed phase reactant species (A_k) and the index of the condensed phase product species (B_k) are specified by the user. The function $g\left(Y_{O_2}\right)$ in Equation 39 is calculated as:

$$g\left(Y_{\mathrm{O}_2}\right)=\begin{cases}1 & \text{for } n_{\mathrm{O}_2,k}=0 \\ \left(1+Y_{\mathrm{O}_2}\right)^{n_{\mathrm{O}_2,k}}-1 & \text{for } n_{\mathrm{O}_2,k}\neq 0 \text{ and } \texttt{IO2TYPE}=0 \\ Y_{\mathrm{O}_2}^{n_{\mathrm{O}_2,k}} & \text{for } n_{\mathrm{O}_2,k}\neq 0 \text{ and } \texttt{IO2TYPE}=1\end{cases} \tag{40}$$

In Equation 40, the oxygen mass fraction (Y_{O_2}) is the local value inside the decomposing solid as determined by solution of the gaseous species conservation equations. It is not the freestream value (except for TGA simulations, i.e. 0D transient formulation). The exponent $n_{O_2,k}$ describes the oxygen sensitivity of reaction *k,* so a value of $n_{O_2,k}=0$ is specified for reactions that are not sensitive to oxygen. The parameter `IO2TYPE` is a user-specified integer that selects via Equation 40 the functional form for the dependence of reaction rate on oxygen concentration is used by Gpyro (see User's Guide).

Each reaction's kinetics are characterized by these parameters: 1) n_k (reaction order in remaining mass of condensed phase species A_k), 2) $n_{O_2,k}$ (reaction order in gaseous oxygen mass fraction), also specify `IO2TYPE`, 3) Z_k (pre–exponential factor), 4) E_k (activation energy), and 5) $T_{crit,k}$.

Equation 39 looks somewhat complicated due to its generality, but it can be simplified for some special cases. When $n_k = 1$ and $n_{O_2,k}=0$, Equation 39 reduces to the following simple form:

$$r_k=\dot{\omega}'''_{dA_k}=\overline{\rho}Y_{A_k}Z_k\exp\left(-\frac{E_k}{RT}\right) \tag{41}$$

Also, for $n_{O_2,k}=0$, $\left(\overline{\rho}Y_i\Delta z\right)_\Sigma$ in Equation 36 replaced with $\left(\overline{\rho}\Delta z\right)\big|_{t=0}$ (conventional reaction order approach), and no volume change (Δz = constant), Equation 39 reduces to:

$$\frac{r_k}{\overline{\rho}\big|_{t=0}}=\frac{\dot{\omega}'''_{dA_k}}{\overline{\rho}\big|_{t=0}}=\left(\frac{\overline{\rho}Y_{A_k}}{\overline{\rho}\big|_{t=0}}\right)^{n_k}Z_k\exp\left(-\frac{E_k}{RT}\right) \tag{42}$$

Equation 42 is the same reaction rate treatment used in NIST's Fire Dynamics Simulator Version 5. Thus, it can be seen that the treatment of pyrolysis reactions in FDS is a special case of the more generalized treatment used in Gpyro.

3.4.1 Specialized reaction models

The reaction rate expression developed in the previous section assumes an n^{th} order reaction model (see Equation 39b). However, several additional reaction models are also available. In particular, by specifying a nonzero value of m_k for reaction k, a multiplicative factor $\alpha_{A_k}^{m_k}$ is added to Equation 39a (recall that for reaction k, the condensed-phase reactant species has index A_k). Also, for each reaction, the user may specify an index `IKINETICMODEL` that invokes a

different functional form of $f(\alpha_{A_k})$ corresponding to various reaction models. The available reaction models are summarized in Table 1.

Table 1. Specialized reaction models.
Reaction model is $\alpha_{A_k}^{m_k} f(\alpha_{A_k})$ where $f(\alpha_{A_k})$ is given below.

IKIETICMODEL	$f(\alpha_{A_k})$	Description
0	$(1-\alpha_{A_k})^{n_k}$	n^{th} order
1	$\frac{1}{n_k}(1-\alpha_{A_k})[-\ln(1-\alpha_{A_k})]^{1-n_k}$	Nucleation and nucleus growing
2	$(1-\alpha_{A_k})^{n_k}$	Phase boundary reaction
3	$\frac{1/2}{\alpha_{A_k}}$	Diffusion – plane symmetry
4	$\frac{1}{-\ln(1-\alpha_{A_k})}$	Diffusion – cylindrical symmetry
5	$\frac{3/2}{(1-\alpha_{A_k})^{-1/3}-1}$	Diffusion – spherical symmetry
6	$-\frac{3}{2}\frac{(1-\alpha_{A_k})^{-1/3}}{\alpha_{A_k}}$	Diffusion – Jander's type
7	$\frac{1}{n_k}\alpha_{A_k}^{1-n_k}$	Potential law
8	$\frac{1}{n_k}(1-\alpha_{A_k})^{1-n_k}$	Reaction order
9	$(1-\alpha_{A_k})^{n_k}(1+K_{cat,k}\alpha_{icat,k})$	Catalytic

Notes:

$$1-\alpha_{A_k}=\frac{\overline{\rho}Y_{A_k}\Delta z}{(\overline{\rho}Y_{A_k}\Delta z)_{\Sigma}}$$

3.5 Heat release/absorption due to heterogeneous reactions

In Gpyro, the total heat of reaction is calculated as the sum of two separate contributions. One part of the heat of reaction applies only to the generation of condensed phase species and is denoted $\Delta H_{sol,k}$ (where *sol* stands for *solid*); the other part applies only to the generation of volatiles from the condensed phase and is denoted $\Delta H_{vol,k}$ (where *vol* stands for *volatiles*). The volumetric rate of heat release or absorption to the solid phase due to reaction *k* is:

$$\dot{Q}_{s,k}'''=\begin{cases}-\dot{\omega}_{fB_k}'''\Delta H_{sol,k}-\dot{\omega}_{fg_k}'''\Delta H_{vol,k} & \text{for } \Delta H_{sol,k}\neq\Delta H_{vol,k}\\ -\dot{\omega}_{dA_k}'''\Delta H_k & \text{for } \Delta H_{sol,k}=\Delta H_{vol,k}=\Delta H_k\end{cases} \tag{43}$$

$\Delta H_{sol,k}$ is the user-specified chemical (not sensible) specific enthalpy difference between condensed phase species B_k and A_k, i.e. $\Delta H_{sol,k} = h^{\circ}_{B_k} - h^{\circ}_{A_k}$ where a superscript $^{\circ}$ denotes chemical (not sensible or total) enthalpy. Recall that reaction k converts condensed phase species A_k to condensed phase species B_k plus gases. The change in sensible enthalpy is accounted for by the $\sum\left(\dot{\omega}'''_{fi} - \dot{\omega}'''_{di}\right)h_i$ term in Equation 151, so it is important to emphasize that $\Delta H_{sol,k}$ does not include sensible enthalpy differences between B_k and A_k. The units of $\Delta H_{sol,k}$ are Joules per kilogram of species B_k produced by reaction k. Positive values of $\Delta H_{sol,k}$ correspond to an endothermic reaction, and negative values correspond to an exothermic reaction. $\Delta H_{sol,k}$ is often set to zero, unless reaction k represents a solid–solid or solid–liquid phase change with an associated change in chemical enthalpy. As will be explained below, $\Delta H_{sol,k}$ may also be nonzero if it is desired to apply a heat of reaction having units Joules per kilogram of condensed phase reactant consumed.

The term $\Delta H_{vol,k}$ is the user-specified quantity of heat required to convert unit mass of condensed-phase species A_k to gases at whatever temperature the reaction occurs. $\Delta H_{vol,k}$ is treated in Gpyro as a user-specified semi-empirical constant because detailed knowledge of the chemical and sensible enthalpies of all gaseous and condensed phase species is required to assign physical/chemical significance to $\Delta H_{vol,k}$: formally, $\Delta H_{vol,k}$ is the total (chemical plus sensible) enthalpy of the gases (h_{T,g_k}) produced by volatilizing condensed-phase species A_k minus the total enthalpy of condensed-phase species A_k (h_{T,A_k}), i.e. $\Delta H_{vol,k} = h_{T,g_k} - h_{T,A_k} = \left(h^{\circ}_{g_k} - h^{\circ}_{A_k}\right) + \left(h_{g_k} - h_{A_k}\right)$. Here, a subscript T denotes total enthalpy. Note that the rightmost parenthetical term is a constant, in general, only if the reaction always occurs at the same temperature (which is not the case for finite-rate reactions) or the solid reactant species A_k has the same specific heat capacity as the product gases.

In a two-temperature formulation, there is some ambiguity regarding the temperature at which the gaseous sensible enthalpy is evaluated (temperature of condensed or gaseous phase). When newly volatilized gases are produced, their temperature is probably very close to the condensed-phase temperature; however, molecular interactions will cause the newly-generated volatiles to quickly approach the temperature of the gas-phase, so it may be more appropriate to evaluate the gas enthalpy in the above equation at the gas-phase temperature. By assuming that the volatiles generated from the condensed phase have a temperature equal to the gas-phase temperature (i.e. the enthalpy of the gas produced from the condensed-phase is evaluated at the gas-phase temperature instead of the condensed-phase temperature) the term $\sum_{j=1}^{N}\left(\dot{\omega}'''_{fj} - \dot{\omega}'''_{dj}\right)h_{g,j} - \dot{\omega}'''_{fg}h_g$ appearing in the gaseous energy equation cancels because $\dot{\omega}'''_{fg} = \sum_{j=1}^{N}\left(\dot{\omega}'''_{fj} - \dot{\omega}'''_{dj}\right)$. This approximation is made by default in Gpyro, but the user can specify `GASES_PRODUCED_AT_TSOLID = .TRUE.` in the `&GPYRO_GENERAL` namelist group to remove this approximation.

Due to the complexities mentioned above, Gpyro by default makes the approximation that ΔH_{vol} is a user-specified constant (implying that $h_{T,g_k} - h_{T,A_k}$ is invariant when in actuality it may vary

with reaction temperature and other factors). A slightly different treatment of the heat of reaction can be invoked by specifying `CONSTANT_DHVOL = .FALSE.` in the `&GPYRO_GENERAL` namelist group, causing the heat of reaction to be calculated as:

$$\dot{Q}'''_{s,k} = -\dot{\omega}'''_{fB_k} \Delta H_{sol,k} - \dot{\omega}'''_{fg_k} \Delta H^{\circ}_{vol,k} - \dot{\omega}'''_{fg_k} \left(h_{g_k} - h_{A_k} \right) \tag{44}$$

In this case, instead of specifying $\Delta H_{vol,k}$, the user specifies $\Delta H^{\circ}_{vol,k}$ (where $\Delta H^{\circ}_{vol,k} = h^{\circ}_{g_k} - h^{\circ}_{A_k}$) and the difference in the sensible enthalpy between the volatilized gases and the condensed-phase species A_k (the rightmost term in the above equation) is explicitly added to the heat of reaction. Note that the gas enthalpy is evaluated at the solid temperature, as if the volatiles are generated at the solid temperature.

$\Delta H_{vol,k}$ (or $\Delta H^{\circ}_{vol,k}$) has units of J/kg of gases volatilized from the condensed phase (species A_k). A positive value of $\Delta H_{vol,k}$ denotes an endothermic reaction, and a negative value of $\Delta H_{vol,k}$ denotes an exothermic reaction. $\Delta H_{vol,k}$ is sometimes called the heat of pyrolysis, heat of volatilization, or heat of vaporization. Note that $\Delta H_{vol,k}$ is different from the heat of gasification (sometimes denoted ΔH_g or L_g), which includes a contribution for the sensible enthalpy required to heat the condensed phase from its initial temperature to its volatilization temperature.

Both $\Delta H_{sol,k}$ and $\Delta H_{vol,k}$ have base units of J/kg, but some clarification is needed regarding Joules per kilogram of what. These quantities are defined per unit mass of product that originated in the condensed phase. That is, the units of $\Delta H_{sol,k}$ are Joules per kg of condensed phase species B_k produced from condensed phase species A_k. Similarly, the units of $\Delta H_{vol,k}$ are Joules per kg of gases generated by volatilizing condensed phase species A_k (or equivalently, Joules per kg of gaseous mass generated that originated in the condensed phase). Note that any mass that originated in the gas phase is not included in this heat of reaction. For example, assume a noncharring reaction converts 1 kg of condensed phase species A and 1 kg of gaseous oxygen to 2 kg of product gases, releasing 1 MJ of sensible enthalpy in the process. The value of $\Delta H_{vol,k}$ for this reaction is –1 MJ/kg, not –1/2 MJ/kg.

In the literature, heats of reaction are sometimes given on a J per kg of *reactant consumed* basis. Using the present terminology, such a heat of reaction would have units of Joules per kilogram of species A_k destroyed by reaction k. This treatment of heats of reaction can be recovered in Gpyro by setting $\Delta H_{sol,k} = \Delta H_{vol,k} = \Delta H_k$. In fact, the second equality in Equation 43 follows from the first equality after setting $\Delta H_{sol,k} = \Delta H_{vol,k} = \Delta H_k$ and then making use of Equation 25:

$$\begin{aligned}
\dot{Q}'''_{s,k} &= -\dot{\omega}'''_{fB_k} \Delta H_{sol,k} - \dot{\omega}'''_{fg_k} \Delta H_{vol,k} \\
&= -\left(\dot{\omega}'''_{fB_k} \Delta H_{sol,k} + \dot{\omega}'''_{fg_k} \Delta H_{vol,k} \right) \\
&= -\left(\dot{\omega}'''_{fB_k} \Delta H_k + \dot{\omega}'''_{fg_k} \Delta H_k \right) \\
&= -\left(\dot{\omega}'''_{fB_k} + \dot{\omega}'''_{fg_k} \right) \Delta H_k \\
&= -\dot{\omega}'''_{dA_k} \Delta H_k
\end{aligned} \tag{45}$$

The flexibility that this affords is the primary motivation for splitting the heat of reaction into two separate components.

Since the source term $\dot{Q}'''_{s,k}$ appears in the condensed phase energy conservation equation (Equation 151), any heat release or absorption due to Equation 43 is distributed to the condensed phase (the subscript *s* denotes "solid" although "condensed" would be more accurate). Whether the heat released or absorbed by a heterogeneous reaction is distributed to the condensed phase or the gas phase is somewhat inconsequential since these phases are usually in a state close to thermal equilibrium on account of the much lower volumetric heat capacity of the gas phase.

3.6 Homogeneous gas phase reactions

In addition to heterogeneous reactions involving the condensed and gaseous phases, the user may also specify any number of homogeneous gas phase reactions. Such reactions can be used to account for tar cracking where large hydrocarbon molecules are broken into smaller hydrocarbon molecules or the oxidation of pyrolysate as it flows through a char layer toward the surface where both the oxygen concentration and temperature are highest.

Just as there are K condensed phase reactions and individual condensed phase reactions are indicated by the index k, there are L homogeneous gas phase reactions and individual reactions are indicated by the index ℓ. Each homogeneous gas phase reaction ℓ converts two gas phase reactants (A_ℓ and B_ℓ) to gaseous products. Since only the gas phase is involved, these reactions are termed "homogeneous" to differentiate them from the heterogeneous reactions discussed earlier.

Although the stoichiometry of gas phase reactions is usually expressed on a molar basis, the stoichiometry of homogeneous gas phase reactions is expressed here on a mass basis:

$$1\,\text{kg } A_\ell - y_{g,B_\ell,\ell}\,\text{kg } B_\ell \rightarrow \sum_{j=1}^{N} \max\left(y_{g,j,\ell},0\right)\text{kg gas } j \tag{46}$$

In Equation 46, $y_{g,j,\ell}$ is the N by L "homogeneous gaseous species yield matrix", analogous to the gaseous species yield matrix ($y_{s,j,k}$) discussed earlier with reference to heterogeneous reactions, and the negative sign on the second term on the LHS is deliberate. The physical meaning of individual entries in $y_{g,j,\ell}$ is the net mass of gaseous species j produced by reaction ℓ (for positive entries) or consumed by reaction ℓ (for negative entries) per unit mass of gaseous species A_ℓ consumed. Note that in writing Equation 46, it is assumed that $y_{g,A_\ell,\ell} = -1$, i.e. the yield corresponding to gas phase species A_ℓ is –1. It is also assumed that for reaction ℓ, the only other negative entry in the $y_{g,j,\ell}$ matrix is the yield corresponding to gas phase species B_ℓ (denoted $y_{g,B_\ell,\ell}$ in Equation 46). This is why there is a negative sign in front of the second term on the LHS of Equation 46. All entries in a column of the homogeneous gaseous species yield matrix must add to 0 for mass to be conserved, and this must be strictly obeyed or nonphysical results will occur. The negative sign in the second term on the LHS is deliberate; it results from the convention that a negative entry in $y_{g,j,\ell}$ causes corresponds to species consumption.

The reaction rate of the ℓ^{th} homogeneous gas phase reaction is the destruction rate of gas phase species A_ℓ:

$$r_\ell = \dot{\omega}'''_{dA_\ell} = \left[A_\ell\right]^{p_\ell}\left[B_\ell\right]^{q_\ell} T^{b_\ell} Z_\ell \overline{\psi} \exp\left(-\frac{E_\ell}{RT_g}\right) \tag{47}$$

In Equation 47, $\dot{\omega}'''_{dA_\ell}$ is the destruction rate of gaseous species A_ℓ due to homogeneous gas phase reaction ℓ, and $[A_\ell]$ denotes the molar concentration of gaseous species A_ℓ:

$$\left[A_\ell\right] = \frac{\rho_g Y_{A_\ell}}{M_{A_\ell}} \tag{48}$$

Note that the entry corresponding to species A_ℓ in the $y_{g,j,\ell}$ matrix must be –1 for the first equality in Equation 47 to be true, and this is consistent with the discussion following Equation 46. Porosity ($\overline{\psi}$) appears in Equation 47 because reaction rates are defined on a per unit volume of solid plus gas (i.e. per unit volume of mixture) basis. For dimensional consistency in Equation 47, the units of Z vary with the specified values of p, q, and b. For p = 1, q = 1, and b = 0, the units of Z are kg–m^3/mole^2–s.

The creation or destruction of gaseous species j by homogeneous gaseous reaction ℓ is calculated from the homogeneous gaseous species yield matrix ($y_{g,j,\ell}$) as:

$$\dot{\omega}'''_{g,fj,\ell} = r_\ell \max\left(y_{g,j,\ell}, 0\right) \tag{49}$$

$$\dot{\omega}'''_{g,dj,\ell} = -r_\ell \min\left(y_{g,j,\ell}, 0\right) \tag{50}$$

Note the analogy to Equations 26 and 27.

Total species formation rates due to homogeneous gaseous reactions are determined by summing over all reactions (note the analogy to Equations 28 and 29):

$$\dot{\omega}'''_{g,dj} = \sum_{\ell=1}^{L} \dot{\omega}'''_{g,dj,\ell} \tag{51}$$

$$\dot{\omega}'''_{g,fj} = \sum_{\ell=1}^{L} \dot{\omega}'''_{g,fj,\ell} \tag{52}$$

The volumetric rate of heat release (or absorption) to the gas phase by homogeneous gaseous reaction ℓ is:

$$\dot{Q}'''_{g,\ell} = -\dot{\omega}'''_{dA_\ell} \Delta H_\ell \tag{53}$$

where ΔH_ℓ is the heat of reaction associated with homogeneous gas phase reaction ℓ. Its units are J of heat released per unit mass of gas phase species A_ℓ consumed by homogeneous gas phase reaction ℓ. As with the condensed phase reactions, positive values of ΔH_ℓ correspond to an endothermic reaction, and negative values correspond to an exothermic reaction. The subscript g in Equation 53 indicates that any heat absorbed or released is distributed to the gas phase.

3.7 Gaseous species total source terms

Gaseous species can be consumed or destroyed in both heterogeneous (solid/gas) and homogeneous (gas/gas) reactions. The source term needed in the gas-phase species conservation equation is obtained by summing the contributions from both types of reaction rates:

$$\dot{\omega}'''_{dj} = \dot{\omega}'''_{s,dj} + \dot{\omega}'''_{g,dj} \tag{54}$$

$$\dot{\omega}'''_{fj} = \dot{\omega}'''_{s,fj} + \dot{\omega}'''_{g,fj} \tag{55}$$

All expressions on the RHS have been defined in Equations 28, 29, 51, and 52.

4.0 GOVERNING EQUATIONS

4.1 One-dimensional (with volume change)

4.1.1 Control volume system

The one-dimensional control volume system from which the governing equations are derived is shown schematically in Figure 1. Cell P ("point") has neighboring cells T ("top") and B ("bottom"). The interface between cell P and T is denoted t, and the interface between cell P and B is denoted b. The notation ϕ_T indicates the value of variable ϕ in cell T and ϕ_t indicates the value of variable ϕ at the interface between P and T. $(\delta z)_t$ is the distance from P to T and $(\delta z)_b$ is the distance from P to B. The size (height) of cell P is $(\Delta z)_P$. For the purpose of calculating source terms, it is assumed that the value of ϕ at the center of a particular cell prevails over the entire cell, but for calculating gradients at cell boundaries it is assumed that ϕ varies in a piecewise linear manner between cell centers. The z dimension increases with depth into the solid, i.e. $z = 0$ corresponds to the surface and $z = \delta$ corresponds to the back face. Note that P is located at the center of each cell, except for the two boundary nodes where P is at the edge (because these are "half" cells). The convention used is that ϕ° denotes the value of ϕ at time t and ϕ denotes the value of ϕ at time $t + \Delta t$. The governing equations are solved using a fully implicit volume formulation.

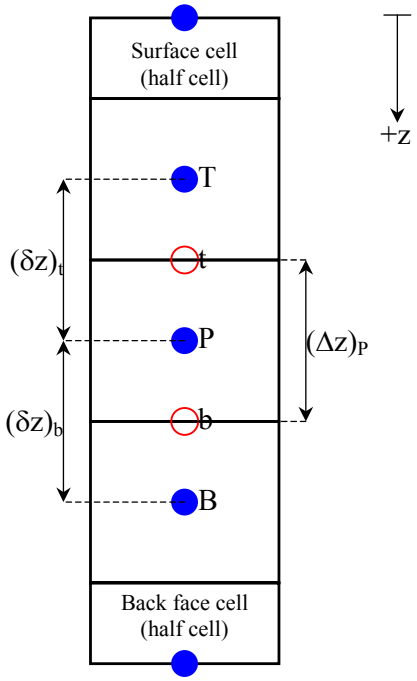

Figure 1. Control volume system used for discretization.

A key aspect of Gpyro is that it is specifically designed to accommodate volume change (shrinkage or swelling). This is accomplished by assuming that bulk density is a property of a condensed phase species and that each grid cell (having height Δz) is permeable to gaseous mass

transfer but is impermeable to condensed phase mass transfer and. Thus, if condensed phase bulk density remains constant but gases escape from a cell (e.g., due to pyrolysis) then Δz decreases to conserve mass (shrinkage). The same shrinkage occurs if no gases escape but the bulk density increases. Conversely, Δz must increase if the bulk density decreases while no gases escape. It is possible to have a release of gases occur simultaneously with a change in bulk density; in this case, the change in Δz, if any, depends on mass conservation. An increase in porosity (decrease in bulk density) can occur with no change in Δz, and this is the usual approach for modeling pyrolysis of charring solids. Due to this formulation, the grid spacing Δz appears in the conservation equations presented below.

4.1.2 Condensed phase mass conservation

The condensed phase mass conservation equation is:

$$\frac{\left(\overline{\rho}\Delta z\right)_P - \left(\overline{\rho}\Delta z\right)_P^{\circ}}{\Delta t} = -\left(\dot{\omega}_{fg}'''\Delta z\right)_P \tag{56}$$

Recall that $\overline{\rho}$ is the weighted bulk density in a vacuum and that Δz is the cell size. No convective terms are present because, as mentioned above, an assumption of Gpyro is that condensed phase mass does not cross cell boundaries (only gaseous mass is permitted to cross cell boundaries). Equation 56 says that the product $\left(\overline{\rho}\Delta z\right)_P$ decreases at a rate proportional to the total volumetric formation rate of all gases from the condensed phase ($\dot{\omega}_{fg}'''$, kg/m^3–s) multiplied by the cell size (Δz). The destruction (consumption) term on the RHS accounts for the conversion of condensed phase mass to gas phase mass, and $\dot{\omega}_{fg}'''$ is defined on a per unit volume of gas plus solid (i.e. per unit volume of mixture) basis. Note that the source term on the RHS is the formation rate of gases from the condensed phase and does not include the formation rate of condensed phase species. This is by design since the formation of one condensed phase species from another, in the absence of gas formation, does not change the quantity $\left(\overline{\rho}\Delta z\right)_P$. Although both $\overline{\rho}$ and Δz could change, their product would be unaffected.

Physically, Equation 56 says that the product of the condensed phase density in a cell and the size of that cell will decrease due to the formation of gases in that cell. For an idealized charring material, the formation of gases will result in a reduction of $\overline{\rho}$ (due to an increase in porosity). Similarly, for an idealized thermoplastic material, the formation of gases will result in a reduction of Δz, i.e. the cell shrinks. For "real" (non–idealized) materials, a reduction of $\overline{\rho}$ may occur simultaneously with a reduction of Δz. As will be discussed below, both $\overline{\rho}$ and Δz are uniquely determined by solving the condensed phase species conservation equation.

4.1.3 Condensed phase species conservation

The condensed phase species conservation equation is similar to the condensed phase mass conservation equation in that it is assumed that no condensed phase species cross cell boundaries:

$$\frac{\left(\overline{\rho} Y_i \Delta z\right)_P - \left(\overline{\rho} Y_i \Delta z\right)_P^\circ}{\Delta t} = \left(\dot{\omega}_{fi}''' \Delta z\right)_P - \left(\dot{\omega}_{di}''' \Delta z\right)_P \tag{57}$$

Here, $\dot{\omega}_{fi}'''$ and $\dot{\omega}_{di}'''$ are, respectively, the volumetric total formation rate and volumetric total destruction rate of condensed phase species *i*. They are defined on a per unit volume of gas plus solid (per unit volume of mixture) basis.

Although it may seem unusual that the grid spacing Δz appears in Equations 56 and 57, these conservation equations are well–posed. Equations 3, 56, and 57 are $M + 2$ equations for $M + 2$ unknowns in each grid cell: the M species' mass fractions, $\overline{\rho}$, and Δz.

4.1.4 Gas phase mass conservation

Unlike Equation 56 (the condensed phase mass conservation equation), the gas-phase mass conservation contains convective terms to account for the flow of volatiles:

$$\frac{\left(\rho_g \overline{\psi} \Delta z\right)_P - \left(\rho_g \overline{\psi} \Delta z\right)_P^\circ}{\Delta t} + \dot{m}''\big|_b - \dot{m}''\big|_t = \left(\dot{\omega}_{fg}''' \Delta z\right)_P \tag{58}$$

The storage term on the LHS is similar to that for the condensed phase mass conservation equation, except the density is that of the gas phase (ρ_g), and the weighted porosity ($\overline{\psi}$) appears. Note that the source term is attributed to the conversion of condensed phase mass to gas phase mass. It is equal in magnitude to, but has the opposite sign of, the source term that appears in the condensed phase mass conservation equation. Porosity does not appear in the source term because, as mentioned above, it is calculated on a per unit volume of mixture (solid plus gas) basis. The only inflow and outflow terms are due to convective mass transfer ($\dot{m}''$) because the diffusive mass transfer terms cancel.

The gas-phase mass conservation equation is explicitly solved only if the pressure solver is not invoked. When the pressure solver is invoked, the gas-phase mass conservation equation is used to form the pressure evolution equation (see Section 4.1.8).

4.1.5 Gas phase species conservation

In the gas phase species conservation equation, both convective and diffusive transport across cell boundaries must be considered. The convective flux of gaseous species *j* is $\dot{m}'' Y_j$ and the diffusive flux of gaseous species *j* is $\dot{j}_j''$. The gas-phase species conservation equation is:

$$\frac{\left(\rho_g \overline{\psi} Y_j \Delta z\right)_P - \left(\rho_g \overline{\psi} Y_j \Delta z\right)_P^\circ}{\Delta t} + \dot{m}'' Y_j\big|_b - \dot{m}'' Y_j\big|_t = -\dot{j}_j''\big|_b + \dot{j}_j''\big|_t + \left(\dot{\omega}_{fj}''' \Delta z\right)_P - \left(\dot{\omega}_{dj}''' \Delta z\right)_P \tag{59}$$

Similar to the condensed phase species conservation equation, $\dot{\omega}_{fj}'''$ is the total formation rate of gaseous species *j* and $\dot{\omega}_{dj}'''$ is the total destruction rate of gaseous species *j*. These terms are defined on a per unit volume of solid plus gas basis, i.e. on a per unit volume of mixture basis. Note that $\dot{\omega}_{fj}'''$ and $\dot{\omega}_{dj}'''$ include contributions from both heterogeneous (gas/solid) and homogeneous (gas/gas) reactions, see Equations 54 and 55.

Although the diffusive term in Equation 144 is written in its general form ($\dot{j}_j''$), Fickian diffusion is assumed:

$$\dot{j}_j'' = -\overline{\psi}\rho_g D\frac{\partial Y_j}{\partial z} \tag{60}$$

4.1.6 Condensed phase energy conservation

The condensed-phase energy conservation equation is:

$$\frac{\left(\overline{\rho}\overline{h}\Delta z\right)_P - \left(\overline{\rho}\overline{h}\Delta z\right)_P^{\circ}}{\Delta t} = -\dot{q}''\Big|_b + \dot{q}''\Big|_t - \left(\dot{Q}_{s-g}'''\Delta z\right)_P + \left(\sum_{k=1}^{K}\dot{Q}_{s,k}'''\Delta z\right)_P - \left(\frac{\partial \dot{q}_r''}{\partial z}\Delta z\right)_P + \sum_{i=1}^{M}\left(\left(\dot{\omega}_{fi}''' - \dot{\omega}_{di}'''\right)h_i\Delta z\right)_P \tag{61}$$

Changes in kinetic energy, potential energy, and work done on the surroundings have been neglected. All source terms are defined on a per unit volume of gas plus solid (i.e. per unit volume of mixture) basis.

Fourier's law is used to calculate $\dot{q}''$, the conductive heat flux through the condensed phase:

$$\dot{q}'' = -\overline{k}\frac{\partial T}{\partial z} \tag{62}$$

The term $\dot{Q}_s'''$ is the volumetric rate of heat release (or absorption) due to condensed phase reactions (see Equation 43). It is obtained by summing over all heterogeneous reactions.

The source term $\dot{Q}_{s-g}'''$ is the volumetric rate of heat transfer from the condensed phase to the gas phase. Note that $\dot{Q}_{g-s}''' = -\dot{Q}_{s-g}'''$, i.e. the rate of heat transfer from the gas to the solid is equal to the negative of the rate of heat transfer from the solid to the gas. Although $\dot{Q}_{s-g}'''$ is sometimes neglected altogether in pyrolysis models on the basis that it is small, Gpyro provides two different options for calculating $\dot{Q}_{s-g}'''$. In the first, thermal equilibrium between the gas-phase and the condensed-phase is assumed. This is called the thermal equilibrium formulation. In the

second, called two-temperature formulation, the rate of heat transfer from the solid to the gas is explicitly calculated. These two formulations can be summarized as:

$$-\dot{Q}'''_{g-s} = \dot{Q}'''_{s-g} = \begin{cases} \dot{m}'' c_{pg} \dfrac{\partial T}{\partial z} - \displaystyle\sum_{\ell=1}^{L} \dot{Q}'''_{g,\ell} & \text{for thermal equilibrium formulation} \\ \\ h_{cv}\left(T - T_g\right) & \text{for two - temperature formulation} \end{cases} \tag{63}$$

Note that $\displaystyle\sum_{\ell=1}^{L} \dot{Q}'''_{g,\ell}$ is the volumetric rate of heat release due to homogeneous gaseous reactions. Essentially, with the thermal equilibrium approach, any heat released by gas-phase reactions is added directly to the solid instead of the gas.

The topmost equality in Equation 63 is obtained by first solving the gas-phase energy conservation equation (presented later as Equation 167b) for $\left(\dot{Q}'''_{s-g}\right)_P$ assuming thermal equilibrium exists between the gaseous and condensed phases, i.e.:

$$\left(\dot{Q}'''_{s-g}\right)_P = \frac{\left(\Delta z\right)^{\circ}_P}{\left(\Delta z\right)_P}\left(\rho_g \overline{\psi}\right)^{\circ}_P \frac{\left(h^*_g\right)_P - \left(h^*_g\right)^{\circ}_P}{\Delta t} + \frac{\left(\dot{m}'' h^*_g\right)_b - \left(\dot{m}'' h^*_g\right)_t}{\left(\Delta z\right)_P} - \left(h^*_g\right)_P \frac{\dot{m}''_b - \dot{m}''_t}{\left(\Delta z\right)_P} - \frac{\left(\overline{\psi}\rho_g D \dfrac{\partial h^*_g}{\partial z}\right)_b - \left(\overline{\psi}\rho_g D \dfrac{\partial h^*_g}{\partial z}\right)_t}{\left(\Delta z\right)_P} - \left(\sum_{\ell=1}^{L} \dot{Q}'''_{g,\ell}\right)_P \tag{64}$$

where h^*_g represents the gas enthalpy evaluated at the condensed-phase temperature, i.e. $h^*_g = c_{pg}\left(T - T_d\right)$. Dropping the subscript P notation, making the approximation that $\left(\Delta z\right)^{\circ}_P / \left(\Delta z\right)_P \approx 1$, and taking the limit as $\Delta t \to 0$ and $\Delta z \to 0$ gives:

$$\begin{aligned} \dot{Q}'''_{s-g} &= \rho_g \overline{\psi} \frac{\partial h^*_g}{\partial t} + \frac{\partial\left(\dot{m}'' h^*_g\right)}{\partial z} - h^*_g \frac{\partial \dot{m}''}{\partial z} - \frac{\partial}{\partial z}\left(\overline{\psi}\rho_g D \frac{\partial h^*_g}{\partial z}\right) - \sum_{\ell=1}^{L} \dot{Q}'''_{g,\ell} \\ &= \rho_g \overline{\psi} c_{pg} \frac{\partial T}{\partial t} + \dot{m}'' c_{pg} \frac{\partial T}{\partial z} - \frac{\partial}{\partial z}\left(\overline{\psi} k_g \frac{\partial T}{\partial z}\right) - \sum_{\ell=1}^{L} \dot{Q}'''_{g,\ell} \\ &\approx \dot{m}'' c_{pg} \frac{\partial T}{\partial z} - \sum_{\ell=1}^{L} \dot{Q}'''_{g,\ell} \end{aligned} \tag{65}$$

where use was made of the definition $k_g = \rho_g D c_{pg}$. Note that this equation assumes thermal equilibrium and therefore all temperatures are condensed-phase temperatures. In writing the last equality, it is assumed that $\rho_g \overline{\psi} c_{pg} << \overline{\rho c}$ and $\overline{\psi} k_g << \overline{k}$.

Gpyro contains an option to use the full expression for $\dot{Q}'''_{s-g}$ (i.e., the middle equality in Equation 65) in thermal equilibrium mode by setting the parameter `FULL_QSG = .TRUE.` on the `&GPYRO_GENERAL` line.

In the second equality in Equation 63, h_{cv} is the volumetric heat transfer coefficient (W/m^3–K). Gpyro provides the ability to specify a constant (independent of Reynolds number and pore characteristics) volumetric heat transfer coefficient, or calculate it from a Nusselt number correlation of the form Nu = a + b Re^c. See the Users Guide for details.

The divergence of the in-depth radiative heat flux vector, treated as a source term, is:

$$\frac{\partial \dot{q}''_r}{\partial z} = -\bar{\varepsilon}\dot{q}''_e\bar{\kappa}(z)\exp\left(-\int_0^z \bar{\kappa}(\zeta)\mathrm{d}\zeta\right) \tag{66}$$

In writing Equation 66 it has been assumed that radiation is applied only normal to the exposed surface and interior radiative emission is not accounted for, i.e. the in–depth radiative heat flux is:

$$\dot{q}''_r(z) = \bar{\varepsilon}\dot{q}''_e \exp\left(-\int_0^z \bar{\kappa}(\zeta)\mathrm{d}\zeta\right) \tag{67}$$

Note that this formulation accounts only for "one–way" radiation, meaning the penetration of radiation into the solid is calculated, but the emission from interior parts of the solid is not calculated (surface radiant emission is still considered, see Equation 111b). This treatment is different from the solid phase model in NIST's Fire Dynamics Simulator Version 5 which accounts for two–way radiation and radiation applied other than normal to the surface. Note that if $\bar{\kappa}$ is not a function of z, then Equation 66 simplifies to $\partial \dot{q}''_r/\partial z = -\bar{\varepsilon}\dot{q}''_e\bar{\kappa}\exp(-\bar{\kappa}z)$.

A decomposing solid frequently consists of a single "layer". However, Gpyro can accommodate materials with a layered or laminated composition. For layers that are not in perfect thermal contact, the rate of heat transfer between layers calculated as $h_{cr}\Delta T$ where h_{cr} is an inverse contact resistance (W/m^2–K) and ΔT is the temperature difference between the "back" of one layer and the "front" of the layer that it abuts. At the interface between two layers that are not in perfect thermal contact, the thermal conductivity $\bar{k}$ in Equation 62 is replaced with $h_{cr}\times\delta z$ where δz is the appropriate distance between cell centers (see Figure 1).

4.1.7 Gas phase energy conservation

The sum of gas-phase conductive and diffusive heat fluxes is:

$$\dot{q}''_g + \sum_{j=1}^{N} \dot{j}''_j h_{g,j} = -\frac{\bar{\psi}k_g}{c_{pg}}\frac{\partial h_g}{\partial z} + \sum_{j=1}^{N}\left(\bar{\psi}\left(\frac{k_g}{c_{pg}} - \rho_g D_j\right)h_{g,j}\frac{\partial Y_j}{\partial z}\right) \tag{68}$$

In Equation 68, Fickian diffusion has been assumed when calculating the diffusive flux term. By making the approximation that all gases have the same diffusion coefficient ($D_j = D$) the summation term in Equation 68 will drop out if $\rho_g D = k_g/c_{pg}$, i.e. by assuming that $k_g = \rho_g c_{pg} D$ (which implies unit Lewis number, Pr = Sc = 1). As mentioned earlier this approximation is made in Gpyro, allowing for considerable simplification:

$$\dot{q}''_g + \sum_{j=1}^{N} \dot{j}''_j h_{g,j} \approx -\overline{\psi}\rho_g D \frac{\partial h_g}{\partial z} \tag{69}$$

With the simplification in Equation 69, the gas-phase energy conservation equation is:

$$\begin{aligned} &\frac{\left(\rho_g \overline{\psi} h_g \Delta z\right)_P - \left(\rho_g \overline{\psi} h_g \Delta z\right)_P^{\circ}}{\Delta t} + \dot{m}'' h_g\Big|_b - \dot{m}'' h_g\Big|_t = \overline{\psi}\rho_g D \frac{\partial h_g}{\partial z}\bigg|_b - \overline{\psi}\rho_g D \frac{\partial h_g}{\partial z}\bigg|_t \\ &+ \left(\dot{Q}'''_{s-g}\Delta z\right)_P + \sum_{k=1}^{K}\left(\left(\dot{\omega}'''_{s,fj,k} h^*_{g,j} - \dot{\omega}'''_{s,dj,k} h_{g,j}\right)\Delta z\right)_P + \left(\sum_{\ell=1}^{L} \dot{Q}'''_{g,\ell}\Delta z\right)_P \end{aligned} \tag{70}$$

Note that h_g^* is the enthalpy of the gas-phase evaluated at the solid-phase temperature, and h_g is the enthalpy of the gas-phase evaluated at the gas-phase temperature. All source terms are defined on a per unit volume of solid plus gas basis, i.e. on a per unit volume of mixture basis. The term $\dot{Q}'''_{s-g}$ is the volumetric rate of heat transfer from the condensed phase to the gas phase (Equation 63).

4.1.8 Gas phase momentum conservation

An equation describing the evolution of the pressure profile inside the decomposing solid is obtained from the gas phase mass conservation equation (Equation 58). Darcian flow with buoyancy is assumed:

$$\dot{m}'' = -\frac{\overline{K}}{\nu}\left(\frac{\partial P}{\partial z} - g\rho_g\right) \tag{71}$$

where the total pressure P is composed of a background pressure (P_0), a flow-induced perturbation pressure (P'), and the hydrostatic gradient ($\rho_\infty g z$):

$$P = P_0 + P' + \rho_\infty g z \tag{72}$$

Substitution of Equation 72 into Equation 71 gives:

$$\dot{m}'' = -\frac{\overline{K}}{\nu}\left(\frac{\partial P'}{\partial z} + g\left(\rho_\infty - \rho_g\right)\right) \tag{73}$$

It can be seen from Equation 73 that if $\partial P'/\partial z = 0$ and $\rho_\infty = \rho_g$ that $\dot{m}'' = 0$, the desired result.

Although one could conceivably solve for the perturbation pressure P' using Equation 73, it is more straightforward to work directly with Equation 71. Consequently, mass flux is related to pressure gradient as:

$$\dot{m}''\big|_b = -\left(\frac{\overline{K}}{\nu}\right)_b \left(\frac{\partial P}{\partial z}\bigg|_b - g\rho_g\big|_b\right) \tag{74a}$$

$$\dot{m}''\big|_t = -\left(\frac{\overline{K}}{\nu}\right)_t \left(\frac{\partial P}{\partial z}\bigg|_t - g\rho_g\big|_t\right) \tag{74b}$$

A pressure evolution equation is obtained by replacing ρ_g with P using the ideal gas law ($P = \rho_g R T_g / \overline{M}$) and substituting Equation 74 into Equation 58:

$$\frac{\left(\frac{P\overline{M}}{RT_g}\overline{\psi}\Delta z\right)_P - \left(\frac{P\overline{M}}{RT_g}\overline{\psi}\Delta z\right)_P^\circ}{\Delta t} = \left(\frac{\overline{K}}{\nu}\right)_b \frac{\partial P}{\partial z}\bigg|_b - \left(\frac{\overline{K}}{\nu}\right)_t \frac{\partial P}{\partial z}\bigg|_t + \left(\dot{\omega}'''_{fg}\Delta z\right)_P - \left(\left(\frac{\overline{K}}{\nu}\rho_g g\right)_b - \left(\frac{\overline{K}}{\nu}\rho_g g\right)_t\right) \tag{75}$$

Equation 75 can be solved for P because all other quantities are calculated elsewhere.

4.2 One-dimensional (no volume change)

For the special case where Δz is fixed, as occurs for charring fuels with no shrinkage or swelling, one can take the limit of the general equations presented earlier as $\Delta t \to 0$ and $\Delta z \to 0$ to obtain partial differential equations. These equations are summarized here:

Condensed-phase mass conservation:

$$\frac{\partial \overline{\rho}}{\partial t} = -\dot{\omega}'''_{fg} \tag{76}$$

Gas-phase mass-conservation:

$$\frac{\partial\left(\rho_g \overline{\psi}\right)}{\partial t} + \frac{\partial \dot{m}''}{\partial z} = \dot{\omega}'''_{fg} \tag{77}$$

Condensed-phase species conservation:

$$\frac{\partial\left(\overline{\rho}Y_i\right)}{\partial t}=\dot{\omega}_{fi}'''-\dot{\omega}_{di}''' \tag{78}$$

Gas-phase species conservation:

$$\frac{\partial\left(\rho_g\overline{\psi}Y_j\right)}{\partial t}+\frac{\partial\left(\dot{m}''Y_j\right)}{\partial z}=-\frac{\partial\dot{j}_j''}{\partial z}+\dot{\omega}_{fj}'''-\dot{\omega}_{dj}''' \tag{79}$$

Condensed-phase energy-conservation:

$$\frac{\partial\left(\overline{\rho}\overline{h}\right)}{\partial t}=-\frac{\partial\dot{q}''}{\partial z}-\dot{Q}_{s-g}'''+\sum_{k=1}^{K}\dot{Q}_{s,k}'''-\frac{\partial\dot{q}_r''}{\partial z}+\sum_{i=1}^{M}\left(\dot{\omega}_{fi}'''-\dot{\omega}_{di}'''\right)h_i \tag{80}$$

Gas-phase energy conservation:

$$\frac{\partial\left(\rho_g\overline{\psi}h_g\right)}{\partial t}+\frac{\partial\left(\dot{m}''h_g\right)}{\partial z}=\frac{\partial}{\partial z}\left(\overline{\psi}\rho_g D\frac{\partial h_g}{\partial z}\right)+\dot{Q}_{s-g}'''+\sum_{k=1}^{K}\left(\dot{\omega}_{s,fj,k}'''h_{g,j}^{*}-\dot{\omega}_{s,dj,k}'''h_{g,j}\right)+\sum_{\ell=1}^{L}\dot{Q}_{g,\ell}''' \tag{81}$$

Pressure evolution equation:

$$\frac{\partial}{\partial t}\left(\frac{P\overline{M}}{RT_g}\overline{\psi}\right)=\frac{\partial}{\partial z}\left(\frac{\overline{K}}{\nu}\frac{\partial P}{\partial z}\right)+\dot{\omega}_{fg}'''-g\frac{\partial}{\partial z}\left(\frac{\overline{K}}{\nu}\rho_g\right) \tag{82}$$

4.3 Two-dimensional (no volume change)

The two-dimensional governing equations are summarized below.

Condensed-phase mass conservation:

$$\frac{\partial\overline{\rho}}{\partial t}=-\dot{\omega}_{fg}''' \tag{83}$$

Gas-phase mass-conservation:

$$\frac{\partial\left(\rho_g\overline{\psi}\right)}{\partial t}+\frac{\partial\dot{m}_z''}{\partial z}+\frac{\partial\dot{m}_x''}{\partial x}=\dot{\omega}_{fg}''' \tag{84}$$

Condensed-phase species conservation:

$$\frac{\partial\left(\overline{\rho}Y_i\right)}{\partial t}=\dot{\omega}_{fi}'''-\dot{\omega}_{di}''' \tag{85}$$

Gas-phase species conservation:

$$\frac{\partial\left(\rho_g\overline{\psi}Y_j\right)}{\partial t}+\frac{\partial\left(\dot{m}_z''Y_j\right)}{\partial z}+\frac{\partial\left(\dot{m}_x''Y_j\right)}{\partial x}=-\frac{\partial\dot{j}_{j,z}''}{\partial z}-\frac{\partial\dot{j}_{j,x}''}{\partial x}+\dot{\omega}_{fj}'''-\dot{\omega}_{dj}''' \tag{86}$$

Condensed-phase energy-conservation:

$$\frac{\partial\left(\overline{\rho}\overline{h}\right)}{\partial t}=-\frac{\partial\dot{q}_z''}{\partial z}-\frac{\partial\dot{q}_x''}{\partial x}-\dot{Q}_{s-g}'''+\sum_{k=1}^{K}\dot{Q}_{s,k}'''-\frac{\partial\dot{q}_r''}{\partial z}+\sum_{i=1}^{M}\left(\dot{\omega}_{fi}'''-\dot{\omega}_{di}'''\right)h_i \tag{87}$$

Gas-phase energy conservation:

$$\begin{aligned}&\frac{\partial\left(\rho_g\overline{\psi}h_g\right)}{\partial t}+\frac{\partial\left(\dot{m}_z''h_g\right)}{\partial z}+\frac{\partial\left(\dot{m}_x''h_g\right)}{\partial x}=\frac{\partial}{\partial z}\left(\overline{\psi}\rho_g D\frac{\partial h_g}{\partial z}\right)+\frac{\partial}{\partial x}\left(\overline{\psi}\rho_g D\frac{\partial h_g}{\partial x}\right)\\&+\dot{Q}_{s-g}'''+\sum_{k=1}^{K}\left(\dot{\omega}_{s,fj,k}'''h_{g,j}^{*}-\dot{\omega}_{s,dj,k}'''h_{g,j}\right)+\sum_{\ell=1}^{L}\dot{Q}_{g,\ell}'''\end{aligned} \tag{88}$$

Pressure evolution equation:

$$\frac{\partial}{\partial t}\left(\frac{P\overline{M}}{RT_g}\overline{\psi}\right)=\frac{\partial}{\partial z}\left(\frac{\overline{K}}{\nu}\frac{\partial P}{\partial z}\right)+\frac{\partial}{\partial x}\left(\frac{\overline{K}}{\nu}\frac{\partial P}{\partial x}\right)+\dot{\omega}_{fg}'''-g\frac{\partial}{\partial z}\left(\frac{\overline{K}}{\nu}\rho_g\right) \tag{89}$$

4.3 Three-dimensional (no volume change)

The three-dimensional governing equations are summarized below.

Condensed-phase mass conservation:

$$\frac{\partial\overline{\rho}}{\partial t}=-\dot{\omega}_{fg}''' \tag{90}$$

Gas-phase mass-conservation:

$$\frac{\partial\left(\rho_g\overline{\psi}\right)}{\partial t}+\frac{\partial\dot{m}_x''}{\partial x}+\frac{\partial\dot{m}_y''}{\partial y}+\frac{\partial\dot{m}_z''}{\partial z}=\dot{\omega}_{fg}''' \tag{91}$$

Condensed-phase species conservation:

$$\frac{\partial\left(\overline{\rho}Y_i\right)}{\partial t}=\dot{\omega}_{fi}'''-\dot{\omega}_{di}''' \tag{92}$$

Gas-phase species conservation:

$$\frac{\partial\left(\rho_g\overline{\psi}Y_j\right)}{\partial t}+\frac{\partial\left(\dot{m}''_x Y_j\right)}{\partial x}+\frac{\partial\left(\dot{m}''_y Y_j\right)}{\partial y}+\frac{\partial\left(\dot{m}''_z Y_j\right)}{\partial z}=-\frac{\partial\dot{j}''_{j,x}}{\partial x}-\frac{\partial\dot{j}''_{j,y}}{\partial y}-\frac{\partial\dot{j}''_{j,z}}{\partial z}+\dot{\omega}'''_{fj}-\dot{\omega}'''_{dj} \tag{93}$$

Condensed-phase energy-conservation:

$$\frac{\partial\left(\overline{\rho}\overline{h}\right)}{\partial t}=-\frac{\partial\dot{q}''_x}{\partial x}-\frac{\partial\dot{q}''_y}{\partial y}-\frac{\partial\dot{q}''_z}{\partial z}-\dot{Q}'''_{s-g}+\sum_{k=1}^{K}\dot{Q}'''_{s,k}-\frac{\partial\dot{q}''_r}{\partial z}+\sum_{i=1}^{M}\left(\dot{\omega}'''_{fi}-\dot{\omega}'''_{di}\right)h_i \tag{94}$$

Gas-phase energy conservation:

$$\begin{aligned}&\frac{\partial\left(\rho_g\overline{\psi}h_g\right)}{\partial t}+\frac{\partial\left(\dot{m}''_x h_g\right)}{\partial x}+\frac{\partial\left(\dot{m}''_y h_g\right)}{\partial y}+\frac{\partial\left(\dot{m}''_z h_g\right)}{\partial z}=\frac{\partial}{\partial x}\left(\overline{\psi}\rho_g D\frac{\partial h_g}{\partial x}\right)+\frac{\partial}{\partial y}\left(\overline{\psi}\rho_g D\frac{\partial h_g}{\partial y}\right)+\\&\frac{\partial}{\partial z}\left(\overline{\psi}\rho_g D\frac{\partial h_g}{\partial z}\right)+\dot{Q}'''_{s-g}+\sum_{k=1}^{K}\left(\dot{\omega}'''_{s,fj,k}h^*_{g,j}-\dot{\omega}'''_{s,dj,k}h_{g,j}\right)+\sum_{\ell=1}^{L}\dot{Q}'''_{g,\ell}\end{aligned} \tag{95}$$

Pressure evolution equation:

$$\begin{aligned}&\frac{\partial}{\partial t}\left(\frac{P\overline{M}}{RT_g}\overline{\psi}\right)=\frac{\partial}{\partial x}\left(\frac{\overline{K}}{\nu}\frac{\partial P}{\partial x}\right)+\frac{\partial}{\partial y}\left(\frac{\overline{K}}{\nu}\frac{\partial P}{\partial y}\right)+\frac{\partial}{\partial z}\left(\frac{\overline{K}}{\nu}\frac{\partial P}{\partial z}\right)+\dot{\omega}'''_{fg}-\\&g_x\frac{\partial}{\partial x}\left(\frac{\overline{K}}{\nu}\rho_g\right)-g_y\frac{\partial}{\partial y}\left(\frac{\overline{K}}{\nu}\rho_g\right)-g_z\frac{\partial}{\partial z}\left(\frac{\overline{K}}{\nu}\rho_g\right)\end{aligned} \tag{96}$$

4.4 Zero-dimensional

Gpyro can solve 0D transient equations that represent the mass and species evolution of a "lumped" particle having negligible gradients of temperature species as occurs in idealized thermal analysis experiments. Zero–dimensional transient forms of the governing equations are presented below.

Condensed phase mass conservation:

$$\frac{\left(\overline{\rho}\Delta z\right)-\left(\overline{\rho}\Delta z\right)^{\circ}}{\Delta t}=-\dot{\omega}'''_{fg}\Delta z \tag{97}$$

Condensed phase species conservation:

$$\frac{\left(\overline{\rho}Y_i\Delta z\right)-\left(\overline{\rho}Y_i\Delta z\right)^{\circ}}{\Delta t}=\dot{\omega}'''_{fi}\Delta z-\dot{\omega}'''_{di}\Delta z \tag{98}$$

Gas phase mass–conservation:

$$\frac{\left(\rho_g \overline{\psi} \Delta z\right) - \left(\rho_g \overline{\psi} \Delta z\right)^{\circ}}{\Delta t} = \dot{\omega}_{fg}''' \Delta z \tag{99}$$

Gas phase species conservation:

$$Y_j = Y_j^{\infty} \tag{100}$$

Condensed phase energy conservation:

$$T = T_0 + \beta t \tag{101}$$

Gas phase energy conservation:

$$T_g = T = T_0 + \beta t \tag{102}$$

Gas phase momentum conservation:

$$P = P_{\infty} \tag{103}$$

Here, β is the linear ramp rate in K/s. The temperature and gas phase mass fractions are taken as the ambient values. Thus, for the 0D transient formulation, T and Y_j are specified by the user rather than calculated. Note that Equations 97 and 98 are essentially the same as the condensed phase mass and species conservation equations presented earlier for cell P in the 1D transient model. Thus, in the 1D transient model, each cell behaves as if it was a single thermogravimetric sample. It is not necessary to solve the gas phase mass conservation equation.

The above governing equations can be used to calculate both differential thermogravimetric curves ($\mathrm{d}/\mathrm{d}t\left(m/m_0\right)$) and thermogravimetric curves (m/m_0). A differential thermogravimetric curve is calculated as:

$$\frac{\mathrm{d}}{\mathrm{d}t}\left(\frac{m''}{m_0''}\right) = -\frac{\dot{\omega}_{fg}''' \Delta z}{m_0''} = -\frac{\dot{\omega}_{fg}''' \Delta z}{\left(\overline{\rho} \Delta z\right)\big|_{t=0}} \tag{104}$$

Integrating the differential thermogravimetric curve gives the thermogravimetric curve:

$$\frac{m''}{m_0''}\left(t\right) = 1 - \frac{1}{m_0''}\int_0^t \dot{\omega}_{fg}'''\left(\tau\right)\Delta z\left(\tau\right)\mathrm{d}\tau \tag{105}$$

Equations 104 and 105 are used primarily for simulating TGA experiments, in particular for extracting decomposition kinetics from TGA data using genetic algorithm optimization. Note that it is not necessary to explicitly solve Equation 99 to calculate TGA curves. The initial conditions on Equations 97 and 98 are the same as those applied to the 1D transient governing equations.

5.0 BOUNDARY AND INITIAL CONDITIONS

NOTE: There is no longer a "default" boundary condition in Gpyro. This will be updated in the next draft.

The default configuration in Gpyro is a 1D formulation representative of a Cone Calorimeter (or similar) experiment. In Section 5.1, the initial and boundary conditions describing this configuration are presented, and in Section 5.2 more general boundary conditions (specified by the BCpatch worksheet) are presented.

5.1 Default – 1D virtual Cone Calorimeter (or similar) experiment

5.1.1 Condensed-phase mass conservation

Equation 56, conservation of condensed-phase mass, reduces to an ordinary differential equation for the quantity $\overline{\rho}\Delta z$ in each cell *P*. Thus, a single initial condition is required in each cell:

$$\left(\overline{\rho}\Delta z\right)^{\circ}\Big|_{t=0} = \overline{\rho}_0\Delta z_0 = \sum_{i=1}^{M}\left(X_{i0}\rho_{i0}\right)\Delta z_0 \tag{106}$$

5.1.2 Condensed-phase species conservation

The condensed phase species conservation equation also reduces to an ODE for the quantity $\overline{\rho}Y_i\Delta z$ in each cell *P*. A single initial condition is required in each cell:

$$\left(\overline{\rho}Y_i\Delta z\right)^{\circ}\Big|_{t=0} = \overline{\rho}_0 Y_{i0}\Delta z_0 = \sum_{i=1}^{M}\left(X_{i0}\rho_{i0}\right)Y_{i0}\Delta z_0 \tag{107}$$

5.1.3 Gas-phase mass conservation

Equation 58, conservation of gas-phase mass, requires one initial condition and one boundary condition. The initial condition in each cell *P* is:

$$\left(\rho_g\overline{\psi}\Delta z\right)^{\circ}\Big|_{t=0} = \rho_{g0}\overline{\psi}_0\Delta z_0 = \sum_{j=1}^{N}\left(X_{j0}\rho_{g,j0}\right)\sum_{i=1}^{M}\left(X_{i0}\psi_{i0}\right)\left(\Delta z\right)_0 \tag{108a}$$

A single boundary condition is required. Normally, this is specification of the mass flux at the back face, which is zero for a negligibly permeable substrate:

$$\dot{m}''\Big|_{z=\delta} = 0 \tag{108b}$$

Note that the gas-phase mass conservation equation is explicitly solved only if the pressure solver is not invoked. When the pressure solver is invoked, the gas-phase mass conservation equation is used as the basis for soliving

5.1.4 Gas-phase species conservation

For each gaseous species *j*, Equation 144 requires one initial and two boundary conditions. The initial conditions in each cell *P* are the gaseous species mass fraction at time $t = 0$:

$$Y_j^\circ\big|_{t=0} = Y_{j0} \tag{109a}$$

Two boundary conditions are required for each gaseous species *j*. Normally, the back face ($z = \delta$) is impermeable so there is no flow of volatiles across the back face and the species mass fraction gradient is set to zero:

$$\left.\frac{\partial Y_j}{\partial z}\right|_{z=\delta} = 0 \tag{109b}$$

No boundary condition is required for gaseous species at an outflow boundary if the Peclet number is sufficiently high [8]. However, this condition is not always met, so the diffusive mass flux of gaseous species into or out of the decomposing solid at the front face is approximated using the heat/mass transfer analogy:

$$-\overline{\psi}\rho_g D\left.\frac{\partial Y_j}{\partial z}\right|_{z=0} \approx \frac{h_c}{c_{pg}}\left(Y_j^\infty - Y_j\big|_{z=0}\right) \tag{109c}$$

If the user desires, the effect of blowing on the heat transfer coefficient can be simulated using a Couette flow approximation [9]:

$$h_c = \frac{\dot{m}_0'' c_{pg}}{\exp\left(\dot{m}_0'' c_{pg} / h_{c,nb}\right) - 1} \tag{110}$$

where $h_{c,nb}$ is the heat transfer coefficient with no blowing, and $\dot{m}_0''$ is the mass flux of gases at the surface. The user specifies whether the heat transfer coefficient is fixed at $h_{c,nb}$, or whether it is reduced due to blowing according to Equation 110.

5.1.5 Condensed-phase energy conservation

One initial and two boundary conditions are required on the condensed-phase energy conservation equation. The initial condition in each cell *P* is:

$$T^\circ\big|_{t=0} = T_0 \qquad \Rightarrow \overline{h}^\circ\big|_{t=0} = \sum_{i=1}^{M}\left(Y_{i0} h_{i0}\left(T_0\right)\right) \tag{111a}$$

The front face boundary condition is:

$$-\bar{k}\left.\frac{\partial T}{\partial z}\right|_{z=0} = \bar{\varepsilon}\dot{q}_e'' - h_c\left(T\big|_{z=0} - T_\infty\right) - \bar{\varepsilon}\sigma\left(T^4\big|_{z=0} - T_\infty^4\right) \quad \text{(for } \bar{\kappa}\big|_{z=0} \to \infty\text{)} \tag{111b}$$

$$-\bar{k}\left.\frac{\partial T}{\partial z}\right|_{z=0} = -h_c\left(T\big|_{z=0} - T_\infty\right) - \bar{\varepsilon}\sigma\left(T^4\big|_{z=0} - T_\infty^4\right) \quad \text{(for } \bar{\kappa}\big|_{z=0} \neq \infty\text{)} \tag{111b}$$

The back face boundary condition is:

$$-\bar{k}\left.\frac{\partial T}{\partial z}\right|_{z=\delta} = h_{c\delta}\left(T\big|_{z=\delta} - T_\infty\right) \tag{111c}$$

5.1.6 Gas-phase energy conservation

One initial and two boundary conditions are required for the gas-phase energy conservation equation. The initial condition in each cell *P* is:

$$T_g^\circ\big|_{t=0} = T_{g0} \quad \Rightarrow \bar{h}_g^\circ\big|_{t=0} = \sum_{j=1}^{N}\left(Y_{j0}h_{g,j}\left(T_0\right)\right)_P = c_{pg}\left(T_{g0} - T_d\right) \tag{112a}$$

The front face boundary condition is:

$$-\bar{\psi}\rho_g D\left.\frac{\partial h_g}{\partial z}\right|_{z=0} = h_c\left(T_\infty - T_g\big|_{z=0}\right) \tag{112b}$$

The back face boundary condition is:

$$-\bar{\psi}\rho_g D\left.\frac{\partial h_g}{\partial z}\right|_{z=\delta} = h_{c\delta}\left(T_g\big|_{z=\delta} - T_\infty\right) \tag{112c}$$

5.1.7 Gas-phase momentum conservation

One initial and two boundary conditions are needed. The initial condition states that the pressure in each cell is atmospheric:

$$P^\circ\big|_{t=0} = P_\infty + \rho_\infty gz \tag{113a}$$

The boundary condition at the front face sets the pressure equal to the atmospheric value:

$$P\big|_{z=0} = P_\infty \tag{113b}$$

The pressure gradient at the back face is set to zero to give an impermeable back face:

$$\left.\frac{\partial P}{\partial z}\right|_{z=\delta} = 0 \tag{113c}$$

5.2 Generalized boundary conditions

This section presents generalized boundary conditions that provide more flexibility than those discussed in Section 5.1. However, the initial conditions remain the same as in Section 5.1.

General boundary conditions are specified over a number of surface "patches". In a 1D simulation, the only available patches are the front face ($z = 0$) and the rear face ($z = \delta$). However, in a 2D simulation, the user may specify different boundary conditions on the edges of the rectangle corresponding to the computational domain. As described in the Users' Guide in greater detail, the user identifies the location of each boundary condition patch by specifying the coordinates x_1, x_2, z_1, and z_2. For example, if the user specifies $x_1 = x_2 = 0.00$ m, $z_1 = 0.01$ m, and $z_2 = 0.02$ m, then Gpyro will apply the specified boundary condition at the plane $x = 0.00$ m for $0.01 \text{ m} < z < 0.02$ m.

In the following sections, the notation s is used to denote the surface "patch" over which the boundary condition is applied. Gradients are written $\partial\phi/\partial n$ where n denotes the coordinate direction that is normal to the patch (i.e., $\partial\phi/\partial n = \partial\phi/\partial x$ for a boundary applied to a constant-x plane, and $\partial\phi/\partial n = \partial\phi/\partial z$ for a boundary applied to a constant-z plane).

5.2.1 Condensed-phase mass conservation

No boundary conditions are required on Equation 56, conservation of condensed-phase mass. The initial condition is already given as Equation 106.

5.2.2 Condensed-phase species conservation

No boundary conditions are required on the condensed phase species conservation equation. The initial condition has already been given as Equation 107.

5.2.3 Gas-phase mass conservation

The initial condition on Equation 58, conservation of gas-phase mass, has already been given as Equation 108b. The single required boundary condition is specification of the mass flux at the back face:

$$\dot{m}''\big|_{z=\delta} = \dot{m}''_{\delta} \tag{114}$$

Recall that the gas-phase mass conservation equation is explicitly solved only if the pressure solver is not invoked. When the pressure solver is invoked, the gas-phase mass conservation equation is used to form the pressure evolution equation (see Section 4.1.8).

5.2.4 Gas-phase species conservation

The initial condition on the gas-phase species conservation equation has already been given as Equation 109a. Two types of gaseous species boundary conditions are available: fixed value and fixed gradient.

A fixed value boundary condition should be applied at inlet boundaries, i.e. the user must specify the composition (mass fractions) of the incoming flow:

$$Y_j\Big|_s = Y_{j\infty} \tag{115}$$

Here, $Y_{j\infty}$ denotes the mass fraction of species j in the incoming flow.

At non-inlet boundaries, a fixed gradient boundary condition can be applied by specifying h_m (a mass transfer coefficient, kg/m^2-s) and Y_j^∞ (the ambient value of each species j). The gaseous species mass fraction gradient at the boundary is then calculated from the following relation:

$$-\overline{\psi}\rho_g D\frac{\partial Y_j}{\partial z}\bigg|_s = h_m\left(Y_j^\infty - Y_j\Big|_s\right) \tag{116}$$

Note that a no flux (zero gradient) boundary condition can be specified by setting $h_m = 0$.

5.2.5 Condensed-phase energy conservation

The initial condition on the condensed-phase energy conservation equation has already been given as Equation 111a.

Two types of boundary conditions may be applied to the condensed-phase energy equation: fixed value (specified temperature), and a radiative-convective balance.

The temperature at a boundary can be directly specified:

$$T\Big|_s = T_{fixed} \tag{117}$$

where T_{fixed} (K) is the specified temperature.

If the user desires a radiative-convective balance, then T_{fixed} should be set to a negative number and the user should specify $\dot{q}_e''$ (externally applied heat flux, W/m^2), h_c (convective heat transfer coefficient, W/m^2-K), and T_∞ (ambient temperature, K). The following boundary condition is then applied:

$$-\bar{k}\left.\frac{\partial T}{\partial z}\right|_s = \bar{\varepsilon}\dot{q}''_e - h_c\left(T\big|_s - T_\infty\right) - \bar{\varepsilon}\sigma\left(T^4\big|_s - T_\infty^4\right) \quad \text{(for } \bar{\kappa}\big|_s \to \infty\text{)} \tag{118a}$$

$$-\bar{k}\left.\frac{\partial T}{\partial z}\right|_s = -h_c\left(T\big|_s - T_\infty\right) - \bar{\varepsilon}\sigma\left(T^4\big|_s - T_\infty^4\right) \quad \text{(for } \bar{\kappa}\big|_s \neq \infty\text{)} \tag{118b}$$

If the user specifies `RERADIATION = .FALSE.` for a particular patch, then the rightmost term on the RHS of Equation 118 is set to zero.

5.2.6 Gas-phase energy conservation

The initial condition on the gas-phase energy conservation equation has already been given as Equation 112a.

As with the condensed-phase energy equation, two types of boundary conditions may be applied to the gas-phase energy equation: fixed value (specified temperature), and a radiative-convective balance.

The gas temperature at a boundary can be directly specified:

$$T_g\big|_s = T_{fixed} \tag{119}$$

where T_{fixed} (K) is the specified gas temperature.

Alternatively, if a radiative-convective balance is desired, then T_{fixed} should be set to a negative number and the user should specify $\dot{q}''_e$ (externally applied heat flux, W/m^2), h_c (convective heat transfer coefficient, W/m^2-K), and T_∞ (ambient temperature, K). The following boundary condition is then applied:

$$-\bar{k}_g\left.\frac{\partial T_g}{\partial z}\right|_s = \bar{\varepsilon}\dot{q}''_e - h_c\left(T_g\big|_s - T_\infty\right) \tag{120}$$

5.2.7 Gas-phase momentum conservation

The initial condition on the gas-phase momentum conservation equation has already been given as Equation 113a.

Two types of boundary conditions are available: fixed value (specified pressure), and fixed gradient (specified mass flux).

If a fixed pressure boundary condition is desired, then the user specifies the pressure at the boundary patch and the following boundary condition is applied:

$$P\big|_s = P_\infty \tag{121}$$

Alternatively, the user may specify a mass flux at a boundary patch, which is implemented numerically by fixing the pressure gradient necessary to give this mass flux:

$$-\frac{\overline{K}}{\nu}\frac{\partial P}{\partial z}\bigg|_s = \dot{m}'' \tag{122}$$

5.4 Geometry masking and initial conditions

In next draft.

5.5 FDS-Gpyro coupling

In next draft.

6.0 NUMERICAL SOLUTION METHODOLOGY

In the previous sections, the governing conservation equations were derived and the treatment of the source terms was presented. In this section, it is explained how these equations are solved numerically. The equations are presented in one-dimensional form for brevity and because extension to two-dimensions is straightforward. However, in Section 6.11 the two-dimensional form of the condensed-phase energy conservation is presented as an example.

6.1 Source term decomposition

In Gpyro, net source terms are partitioned into positive and negative components for numerical convenience. A net source term is the sum of formation (or production) rates and destruction (or absorption) rates. The advantage of decomposing net source terms into its positive and a negative parts is that quantities which, from physical considerations, must remain positive can be prevented from inadvertently becoming negative (see Patankar [8] pg. 145). This is explained in greater detail below.

Consider a source–dominated conservation equation of the same form as Equation 57 where the net source term $\left(S_\phi\right)_P$ is filtered into its positive and negative components:

$$\frac{\phi_P - \phi_P^\circ}{\Delta t} = \left(S_\phi\right)_P = \left(S_\phi^+\right)_P - \left(S_\phi^-\right)_P \tag{123}$$

Here, $\left(S_\phi^+\right)_P \geq 0$, $\left(S_\phi^-\right)_P \geq 0$, and $\left(S_\phi\right)_P = \left(S_\phi^+\right)_P - \left(S_\phi^-\right)_P$. Now multiply the second term on the RHS by ϕ_P/ϕ_P and rearrange:

$$\phi_P = \frac{\dfrac{\phi_P^\circ}{\Delta t} + \left(S_\phi^+\right)_P}{\dfrac{1}{\Delta t} + \dfrac{\left(S_\phi^-\right)_P}{\phi_P}} \tag{124}$$

In practice, to prevent division by zero, this is implemented as:

$$\phi_P = \frac{\dfrac{\phi_P^\circ}{\Delta t} + \left(S_\phi^+\right)_P}{\dfrac{1}{\Delta t} + \dfrac{\left(S_\phi^-\right)_P}{\max\left(\phi_P, \varepsilon\right)}} \tag{125}$$

where ε is a very small number. Note that all quantities on the RHS are greater than or equal to zero. Thus, ϕ_p can approach zero, but it can never become negative. Treating mass and species conservation in this way was found to be critical for ensuring a stable solution.

6.2 Convective-diffusive solver

As will be shown below, the governing equations are discretized in the general form:

$$a_P \phi_P = a_B \phi_B + a_T \phi_T + b \tag{126}$$

For conservation equations involving convection and diffusion, the general form of the a_B and a_T coefficients in Equation 126 are:

$$a_B = \mathsf{D}_b A\left(\left|P_b\right|\right) + \max\left(-F_b, 0\right) \tag{127a}$$

$$a_T = \mathsf{D}_t A\left(\left|P_t\right|\right) + \max\left(-F_t, 0\right) \tag{127b}$$

where the following definitions apply:

$$\mathsf{D}_b = \Gamma_b / \left(\delta z\right)_b \tag{127c}$$

$$\mathsf{D}_t = \Gamma_t / \left(\delta z\right)_t \tag{127d}$$

$$P_b = F_b / \mathsf{D}_b \tag{127e}$$

$$P_t = F_t / \mathsf{D}_t \tag{127f}$$

$$F_b = \dot{m}''\big|_b \tag{127g}$$

$$F_t = \dot{m}''\big|_t \tag{127h}$$

In Equation 127, Γ is a diffusion coefficient (its units and physical significance depends on the equation being solved), P is the cell Peclet number (not pressure), and F is the convective mass flux. The function $A(|P|)$ is given by Patankar [8] in Table 5.2 and repeated below in Table 2:

Table 2. The function $A(|P|)$ from Patankar [8].

	Scheme	Formula for $A(\|P\|)$
1	Central difference	$1 - 0.5\|P\|$
2	Upwind	1
3	Hybrid	$\max(0, 1 - 0.5\|P\|)$
4	Power law	$\max(0, (1 - 0.1\|P\|)^5)$
5	Exponential	$\|P\| / [\exp(P) - 1]$

Since the diffusion coefficient is required at the interface between cells, the interface value is calculated using the harmonic mean between cell P and the adjacent cells (B or T):

$$\Gamma_t = \frac{\Gamma_P \Gamma_T}{\Gamma_T + \frac{(\Delta z)_T (\Gamma_P - \Gamma_T)}{(\Delta z)_P + (\Delta z)_T}} \tag{128a}$$

$$\Gamma_b = \frac{\Gamma_P \Gamma_B}{\Gamma_B + \frac{(\Delta z)_B (\Gamma_P - \Gamma_B)}{(\Delta z)_P + (\Delta z)_B}} \tag{128b}$$

6.2 Tri–diagonal matrix (Thomas) algorithm

Writing the governing equations in the form of Equation 126 makes it possible to use the efficient recursive algorithm known as the Thomas (or tri–diagonal matrix) algorithm. First, rewrite Equation 126 as:

$$a_i \phi_i = b_i \phi_{i+1} + c_i \phi_{i-1} + d_i \tag{129}$$

i.e., a_i is a_P, b_i is a_B, c_i is a_T, and d_i is b. Next, define:

$$P_i = \frac{b_i}{a_i - c_i P_{i-1}} \tag{130a}$$

$$Q_i = \frac{d_i + c_i Q_{i-1}}{a_i - c_i P_{i-1}} \tag{130b}$$

The Thomas algorithm begins by calculating P_1 and Q_1 (where the subscript 1 denotes that these values refer to the first cell):

$$P_1 = \frac{b_1}{a_1} \tag{131a}$$

$$Q_1 = \frac{d_1 + c_1 \phi_0}{a_1} \tag{131b}$$

In Equation 131b, ϕ_0 is the ambient value of ϕ (the subscript 0 denotes the 0^{th} cell). Next, Equations 130a and 130b are used to calculate P_i and Q_i for i = 2 to n where n is the number of cells. The value of ϕ in cell n is calculated as:

$$\phi_n = Q_n + \frac{b_n \phi_{n+1}}{a_n - c_n P_{n-1}} \tag{132}$$

In Equation 132, ϕ_{n+1} represents the value of ϕ flowing into the back face (or the ambient value of ϕ at the back face). With ϕ_n known, the remaining $n-1$ ϕ values are calculated using the relation:

$$\phi_i = P_i \phi_{i+1} + Q_i \tag{133}$$

Some clarification is warranted regarding the coefficients in cell 1 and cell n. Since the TDMA solver is used to solve four separate conservation equations (gaseous species, condensed and gaseous energy, and gaseous momentum) the meaning of the boundary coefficients for each of these conservation equations is discussed separately below.

A fixed value boundary condition at the front face is implemented by specifying $a_1 = 1$, $b_1 = 0$, $c_1 = 0$, and $d_1 = \phi_0$. Similarly, a fixed value boundary condition at the rear face is implemented by specifying $a_n = 1$, $b_n = 0$, $c_n = 0$, and $d_n = \phi_{n+1}$.

A specified mass flux is achieved by setting the pressure gradient to a desired value. The discretized equations at the front and back faces are:

$$\dot{m}_0'' = -\left(\frac{\overline{K}}{\nu} \frac{\partial P}{\partial z} \right)\Bigg|_{z=0} \approx -b_1 \left(P_2 - P_1 \right) \tag{134a}$$

$$\dot{m}_\delta'' = -\left(\frac{\overline{K}}{\nu} \frac{\partial P}{\partial z} \right)\Bigg|_{z=\delta} \approx -c_n \left(P_n - P_{n-1} \right) \tag{134a}$$

It follows from Equation 134a that $P_1 = P_2 + \dot{m}_0''/b_1$ and from Equation 134b that $P_n = P_{n-1} - \dot{m}_\delta''/c_n$. Note that flow into the back face corresponds to a negative value of $\dot{m}''$ and flow into the front face corresponds to a positive value of $\dot{m}''$. The discretized pressure evolution equation at the front and back face is:

$$a_1 P_1 = b_1 P_2 + c_1 P_0 + d_1 \tag{135a}$$

$$a_n P_n = b_n P_{n+1} + c_n P_{n-1} + d_n \tag{135b}$$

Setting $b_n = 0$ and $c_1 = 0$, and substituting Equation 134 into Equation 135 gives expressions for a_1 and a_n:

$$a_1 = \frac{b_1 P_2 + d_1}{P_2 + \dfrac{\dot{m}_0''}{b_1}} \tag{136a}$$

$$a_n = \frac{c_n P_{n-1} + d_n}{P_{n-1} - \dfrac{\dot{m}''_\delta}{c_n}} \tag{136b}$$

A forced mass flux boundary condition is implemented by setting the value of a_1 or a_n per Equation 136.

In the condensed phase energy equation, the convective and radiative losses (or gains) are converted to volumetric source terms by dividing a flux by the boundary node grid size. For example, the convective loss or gain at the front face is accounted for by adding a source term of magnitude $\dot{q}''_c/(\Delta z)_1$ to the source term in cell 1, where $\dot{q}''_c = h_c(T_\infty - T_1)$. Rather than explicitly setting the temperature gradient at the front and back faces, the coefficients c_1 and b_n are set to zero, and volumetric source terms are added to cells 1 and n. Numerically, this is equivalent to explicitly specifying the gradient at the front and back faces, but it is conceptually easier to implement.

In the gas phase species conservation equation, the meanings of c_1 and b_n require careful interpretation. Tracing backward from Equation 129 to Equation 126 to Equation 127, it is seen that $c_1 \equiv a_{T,1} \equiv \mathsf{D}_{t,1} A(|P_{t,1}|) + \max(-F_{t,1}, 0)$ and $b_n \equiv a_{B,n} \equiv \mathsf{D}_{b,1} A(|P_{b,n}|) + \max(-F_{b,n}, 0)$. The usual definition of D_t and D_b are $\mathsf{D}_t = \rho_g \overline{\psi} D/(\delta z)_t$ and $\mathsf{D}_b = \rho_g \overline{\psi} D/(\delta z)_b$. However, in cell 1 and cell n, the heat/mass transfer analogy is used to calculate the value of $\mathsf{D}_{t,1}$ and $\mathsf{D}_{b,n}$ as:

$$\mathsf{D}_{t,1} = h_m \approx \frac{h_c}{c_{pg}} \tag{137a}$$

$$\mathsf{D}_{b,n} = h_m \approx \frac{h_c}{c_{pg}} \tag{137b}$$

The boundary conditions on the gas phase energy conservation equation are implemented in a way that is directly analogous to the gas phase species conservation equation.

6.3 Convergence criteria and relaxation

Due to nonlinearity in the governing equations, a fully–implicit iterative numerical solution is used. Convergence is achieved when the solution in every grid cell chances by less than some predetermined tolerance. Relative tolerances are used to check convergence of the gas phase and condensed phase species equations. For example, the condensed phase species conservation equation is converged when the following is true in every grid cell:

$$\frac{Y_i - Y_{i,old}}{\min(Y_{i,old}, \varepsilon)} < rtol \tag{138}$$

where *rtol* is a user–specified relative tolerance, and ε is a small number to prevent division by zero. Note that $Y_{i,old}$ is the mass fraction at the previous iteration (not the previous time step).

For the other equations, an absolute tolerance is used as the convergence criterion. For example, the pressure evolution equation is converged when the following is true in every grid cell:

$$P - P_{old} < atol \tag{139}$$

where *atol* is a user–specified absolute convergence criterion. Again, P_{old} is the pressure at the previous iteration, not the previous time step.

In order to reduce the possibility of divergence between iterations, solution relaxation is implemented by replacing the coefficients a_P and b in the discretized governing equations with $a_{P,relax}$ and b_{relax}, as shown in Equation 140:

$$a_{P,relax}\phi_P = a_B\phi_B + a_T\phi_T + b_{relax} \tag{140a}$$

$$a_{P,relax} = \frac{a_P}{\alpha} \tag{140b}$$

$$b_{relax} = b + \left(\frac{1-\alpha}{\alpha}\right)a_P\phi_{P,old} \tag{140c}$$

where α is the user–specified relaxation parameter ($0 < \alpha \le 1$) and $\phi_{P,old}$ is the value of ϕ from the previous iteration (not the previous time step). Note that when $\alpha = 1$, $a_{P,relax} = a_P$ and $b_{relax} = b$. For simplicity, the same value of α is applied to all equations and α is static, meaning that it is not dynamically determined during a simulation. Normally, $\alpha = 1$ and solution relaxation via Equation 140 would be invoked only when the solution fails to converge within a pre–determined number of iterations.

6.4 Condensed phase mass conservation

The condensed phase mass conservation equation has been given as Equation 56 and is repeated below:

$$\frac{\left(\overline{\rho}\Delta z\right)_P - \left(\overline{\rho}\Delta z\right)_P^{\circ}}{\Delta t} = -\left(\dot{\omega}_{fg}'''\Delta z\right)_P$$

Note that this is essentially an ODE for the quantity $\overline{\rho}\Delta z$. Thus, no boundary conditions are required; only an initial condition in each cell is required, see Equation 106. Physical considerations require that $\overline{\rho}\Delta z \ge 0$. To ensure that the quantity $\overline{\rho}\Delta z$ remains positive (see Section 6.1), the condensed phase mass conservation equation is integrated in time as:

$$\left(\overline{\rho}\Delta z\right)_P = \frac{\frac{\left(\overline{\rho}\Delta z\right)_P^\circ}{\Delta t}}{\frac{1}{\Delta t} + \frac{\left(\dot{\omega}_{fg}'''\Delta z\right)_P}{\max\left(\left(\overline{\rho}\Delta z\right)_P, \varepsilon\right)}} \tag{141}$$

To prevent numerical difficulties that occur as $\Delta z \to 0$ (as occurs when a slab of a noncharring polymer burns completely away), if a cell's thickness decreases below a user–specified value, then all reaction rates in that cell are set to zero and that cell behaves as if it was inert. Although no numerical problems are encountered as the cell size gets large, the solution is not necessarily accurate if gradients are not well–resolved due to large grid sizes.

6.5 Condensed phase species conservation

The condensed phase species conservation equation has been given as Equation 57:

$$\frac{\left(\overline{\rho}Y_i\Delta z\right)_P - \left(\overline{\rho}Y_i\Delta z\right)_P^\circ}{\Delta t} = \left(\dot{\omega}_{fi}'''\Delta z\right)_P - \left(\dot{\omega}_{di}'''\Delta z\right)_P$$

This is essentially an ODE for the quantity $\overline{\rho}Y_i\Delta z$ in each cell *P*. Thus, no boundary conditions are required, and only an initial condition in each cell is required, see Equation 107.

Physical considerations require $\overline{\rho}Y_i\Delta z \geq 0$. To ensure that $\overline{\rho}Y_i\Delta z$ remains positive (see Section 6.1), numerical solution of the condensed phase species conservation equation is implemented as:

$$\left(\overline{\rho}Y_i\Delta z\right)_P = \frac{\frac{\left(\overline{\rho}Y_i\Delta z\right)_P^\circ}{\Delta t} + \left(\dot{\omega}_{fi}'''\Delta z\right)_P}{\frac{1}{\Delta t} + \frac{\left(\dot{\omega}_{di}'''\Delta z\right)_P}{\max\left(\left(\overline{\rho}Y_i\Delta z\right)_P, \varepsilon\right)}} \tag{142}$$

Here $\dot{\omega}_{fi}'''$ is the total formation rate of condensed phase species *i* (obtained by summing over all reactions *k*) and is positive. Similarly, $\dot{\omega}_{di}'''$ is the total destruction rate of condensed phase species *i* (obtained by summing over all reactions *k*) and is also positive. Since all quantities on the right hand side are greater than or equal to zero, this treatment ensures that the quantity $\overline{\rho}Y_i\Delta z$ does not become negative.

In each grid cell, Equation 141 is solved for $\overline{\rho}\Delta z$. Similarly, each of the *M* values of $\overline{\rho}\Delta z Y_i$ are determined from Equation 142. Then, each Y_i is obtained by dividing $\overline{\rho}\Delta z Y_i$ by $\overline{\rho}\Delta z$. The weighted bulk density $\overline{\rho}$ is then calculated from Equation 3. With $\overline{\rho}$ known, Δz can be determined by dividing $\overline{\rho}\Delta z$ by $\overline{\rho}$. Thus, it can be seen how Y_i, $\overline{\rho}$, and Δz are independently determined from solution of Equations 141 and 142 using the auxiliary relation in Equation 3.

6.6 Gas phase mass conservation

The gas phase mass conservation equation has been given as Equation 58:

$$\frac{\left(\rho_g \overline{\psi} \Delta z\right)_P - \left(\rho_g \overline{\psi} \Delta z\right)_P^\circ}{\Delta t} + \dot{m}''\big|_b - \dot{m}''\big|_t = \left(\dot{\omega}_{fg}''' \Delta z\right)_P$$

This equation (at least in the above form) is explicitly solved only when the pressure solver is not used to calculate $\dot{m}''$. If this is the case, then the gas phase mass conservation equation is used to calculate $\dot{m}''$ assuming that all volatiles generated in–depth escape instantaneously with no resistance to mass transfer, i.e. the mass flux at the top of cell *P* is calculated as:

$$\dot{m}''\big|_t = \dot{m}''\big|_b - \left(\dot{\omega}_{fg}''' \Delta z\right)_P + \frac{\left(\rho_g \overline{\psi} \Delta z\right)_P - \left(\rho_g \overline{\psi} \Delta z\right)_P^\circ}{\Delta t} \tag{143}$$

Thus, provided that $\dot{m}''$ is known at the back face, $\dot{m}''$ can be determined at any point in the decomposing material by applying Equation 143 in every cell starting at the back face and moving toward the front face. Note that due to the coordinate system used (*z* increases with depth into the decomposing solid) $\dot{m}''$ is negative when the flow direction is toward the surface.

6.7 Gas phase species conservation

The final form of the gas phase species conservation equation solved by Gpyro is obtained by multiplying the gas phase mass conservation equation (Equation 58) by $Y_{j,P}$ and subtracting the result from Equation 59. This results in the following equation:

$$\begin{aligned} &\left(\rho_g \overline{\psi} \Delta z\right)_P^\circ \frac{Y_{j,P} - Y_{j,P}^\circ}{\Delta t} + \dot{m}'' Y_j\big|_b - \dot{m}'' Y_j\big|_t - Y_{j,P} \dot{m}''\big|_b + Y_{j,P} \dot{m}''\big|_t = \\ &- \dot{j}_j''\big|_b + \dot{j}_j''\big|_t + \left(\dot{\omega}_{fj}''' \Delta z\right)_P - \left(\dot{\omega}_{dj}''' \Delta z\right)_P - \left(\dot{\omega}_{fg}''' Y_j \Delta z\right)_P \end{aligned} \tag{144}$$

The discretization of and numerical solution of Equation 144 follows Patankar [8]. Begin by defining the following:

$$J_b = \dot{m}'' Y_j\big|_b + \dot{j}_j''\big|_b \tag{145a}$$

$$J_t = \dot{m}'' Y_j\big|_t + \dot{j}_j''\big|_t \tag{145b}$$

$$a_P^\circ = \frac{\left(\Delta z \rho_g \overline{\psi}\right)_P^\circ}{\Delta t} \tag{145e}$$

Substituting Equation 145 into Equation 144 (and multiplying $\left(\dot{\omega}_{dj}''' \Delta z\right)_P$ by $Y_{j,P}/Y_{j,P}$) gives:

$$a_P^\circ\left(Y_{j,P}-Y_{j,P}^\circ\right)+\left(J_b-Y_{j,P}F_b\right)-\left(J_t-Y_{j,P}F_t\right)=$$
$$\left(\dot{\omega}_{fj}'''\Delta z\right)_P-\frac{\left(\dot{\omega}_{dj}'''\Delta z\right)_P}{Y_{j,P}}Y_{j,P}-Y_{j,P}\left(\dot{\omega}_{fg}'''\Delta z\right)_P \tag{146}$$

Following Patankar [8] Equation 5.54–5.55:

$$J_b-Y_{j,P}F_b=a_B\left(Y_{j,P}-Y_{j,B}\right) \tag{147a}$$

$$J_t-Y_{j,P}F_t=a_T\left(Y_{j,T}-Y_{j,P}\right) \tag{147b}$$

Substituting Equation 147 into Equation 146 gives:

$$a_P^\circ\left(Y_{j,P}-Y_{j,P}^\circ\right)+a_B\left(Y_{j,P}-Y_{j,B}\right)-a_T\left(Y_{j,T}-Y_{j,P}\right)=$$
$$\left(\dot{\omega}_{fj}'''\Delta z\right)_P-\frac{\left(\dot{\omega}_{dj}'''\Delta z\right)_P}{Y_{j,P}}Y_{j,P}-Y_{j,P}\left(\dot{\omega}_{fg}'''\Delta z\right)_P \tag{148}$$

Define:

$$b=a_P^\circ Y_{j,P}^\circ+\left(\dot{\omega}_{fj}'''\Delta z\right)_P \tag{149a}$$

$$a_p=a_P^\circ+a_B+a_T+\frac{\left(\dot{\omega}_{dj}'''\Delta z\right)_P}{Y_{j,P}}+\left(\dot{\omega}_{fg}'''\Delta z\right)_P \tag{149b}$$

The final form of the discretized equation is obtained by substituting Equation 149 into Equation 148:

$$a_pY_{j,P}=a_BY_{j,B}+a_TY_{j,T}+b \tag{150}$$

The coefficients a_B and a_T are obtained from Equation 127 by substituting $\Gamma=\rho_g\psi D$.

6.8 Condensed phase energy conservation

To facilitate numerical solution, the final form of the condensed phase energy equation that is solved by Gpryo is obtained by multiplying the condensed phase mass conservation equation (Equation 56) by $\overline{h}_P$ and subtracting the result from Equation 61:

$$\left(\bar{\rho}\Delta z\right)_P^\circ \frac{\bar{h}_P - \bar{h}_P^\circ}{\Delta t} = -\dot{q}''\Big|_b + \dot{q}''\Big|_t - \left(\dot{Q}'''_{s-g}\Delta z\right)_P + \left(\sum_{k=1}^{K}\dot{Q}'''_{s,k}\Delta z\right)_P$$
$$-\left(\frac{\partial \dot{q}''_r}{\partial z}\Delta z\right)_P + \sum_{i=1}^{M}\left(\left(\dot{\omega}'''_{fi} - \dot{\omega}'''_{di}\right)h_i\Delta z\right)_P + \bar{h}_P\left(\dot{\omega}'''_{fg}\Delta z\right)_P \tag{151}$$

Equation 151 can be written as:

$$\left(\bar{\rho}\Delta z\right)_P^\circ \frac{\bar{h}_P - \bar{h}_P^\circ}{\Delta t} = \dot{q}''\Big|_t - \dot{q}''\Big|_b + \left(S\Delta z\right)_P \tag{152a}$$

$$\left(S\right)_P = \left(\sum_{k=1}^{K}\dot{Q}'''_{s,k}\Delta z\right)_P - \left(\frac{\partial \dot{q}''_r}{\partial z}\right)_P + \sum_{i=1}^{M}\left(\left(\dot{\omega}'''_{fi} - \dot{\omega}'''_{di}\right)h_i\right)_P + \bar{h}_P\left(\dot{\omega}'''_{fg}\right)_P - \dot{Q}'''_{s-g} \tag{152b}$$

Where $\dot{Q}'''_{s-g}$ is calculated per Equation 63. For numerical convenience, the source term (Equation 152b) is split into its positive and negative components:

$$S_P = \left(S^+\right)_P - \left(S^-\right)_P \tag{153a}$$

$$\left(S^+\right)_P = h_{cv}T_{g,P} - \left(\frac{\partial \dot{q}''_r}{\partial z}\right)_P + \sum_{i=1}^{M}\left(\dot{\omega}'''_{fi}h_i\right)_P + \bar{h}_P\left(\dot{\omega}'''_{fg}\right)_P + \sum_{k=1}^{K}\max\left(\dot{Q}'''_{s,k},0\right) + \max\left(\dot{Q}'''_{s-g},0\right) \tag{153b}$$

$$\left(S^-\right)_P = h_{cv}T_P + \sum_{i=1}^{M}\left(\dot{\omega}'''_{di}h_i\right)_P - \sum_{k=1}^{K}\min\left(\dot{Q}'''_{s,k},0\right) - \min\left(\dot{Q}'''_{s-g},0\right) \tag{153c}$$

To facilitate use of the efficient Thomas algorithm/TDMA solver to solve Equation 152, the heat conduction terms must be expressed in terms of enthalpy, i.e.:

$$\begin{aligned}\dot{q}''\Big|_t &= -\bar{k}_t\frac{\partial T}{\partial z}\Big|_t \equiv -\left(\frac{\bar{k}}{\bar{c}}\right)_t\left(\frac{\partial \bar{h}}{\partial z}\Big|_t - \sum_{i=1}^{M}\left(h_i\frac{\partial Y_i}{\partial z}\right)_t\right)\\ &\approx -\left(\frac{\bar{k}}{\bar{c}}\right)_t\frac{\bar{h}_P - \bar{h}_T}{\left(\delta z\right)_t} + \sum_{i=1}^{M}\left[\left(\frac{\bar{k}}{\bar{c}}h_i\right)_t\frac{Y_{i,P} - Y_{i,T}}{\left(\delta z\right)_t}\right]\end{aligned} \tag{154a}$$

$$\begin{aligned}\dot{q}''\Big|_b &= -\bar{k}_b\frac{\partial T}{\partial z}\Big|_b \equiv -\left(\frac{\bar{k}}{\bar{c}}\right)_b\left(\frac{\partial \bar{h}}{\partial z}\Big|_b - \sum_{i=1}^{M}\left(h_i\frac{\partial Y_i}{\partial z}\right)_b\right)\\ &\approx -\left(\frac{\bar{k}}{\bar{c}}\right)_b\frac{\bar{h}_B - \bar{h}_P}{\left(\delta z\right)_b} + \sum_{i=1}^{M}\left[\left(\frac{\bar{k}}{\bar{c}}h_i\right)_b\frac{Y_{i,B} - Y_{i,P}}{\left(\delta z\right)_b}\right]\end{aligned} \tag{154b}$$

Substituting Equations 153 and 154 into Equation 152 gives:

$$\frac{\left(\overline{\rho}\Delta z\right)_P^\circ}{\Delta t}\left(\overline{h}_P-\overline{h}_P^\circ\right)=-\left(\frac{\overline{k}}{\overline{c}}\right)_t\frac{\overline{h}_P-\overline{h}_T}{\left(\delta z\right)_t}+\sum_{i=1}^{M}\left[\left(\frac{\overline{k}}{\overline{c}}h_i\right)_t\frac{Y_{i,P}-Y_{i,T}}{\left(\delta z\right)_t}\right]+$$
$$\left(\frac{\overline{k}}{\overline{c}}\right)_b\frac{\overline{h}_B-\overline{h}_P}{\left(\delta z\right)_b}-\sum_{i=1}^{M}\left[\left(\frac{\overline{k}}{\overline{c}}h_i\right)_b\frac{Y_{i,B}-Y_{i,P}}{\left(\delta z\right)_b}\right]+\left(S^+\Delta z\right)_P-\left(S^-\Delta z\right)_P \tag{155}$$

Define:

$$a_P^\circ=\frac{\left(\overline{\rho}\Delta z\right)_P^\circ}{\Delta t} \tag{156a}$$

$$a_T=\frac{\left(\overline{k}/\overline{c}\right)_t}{\left(\delta z\right)_t} \tag{156b}$$

$$a_B=\frac{\left(\overline{k}/\overline{c}\right)_b}{\left(\delta z\right)_b} \tag{156c}$$

$$a_{Th_i}=\frac{\left(\overline{k}h_i/\overline{c}\right)_t}{\left(\delta z\right)_t} \tag{156d}$$

$$a_{Bh_i}=\frac{\left(\overline{k}h_i/\overline{c}\right)_b}{\left(\delta z\right)_b} \tag{156e}$$

The coefficients in the numerator of Equations 156b –156e are calculated using harmonic means (see Equation 128). Substitute Equation 156 into Equation 155:

$$a_P^\circ\left(\overline{h}_P-\overline{h}_P^\circ\right)=-a_T\left(\overline{h}_P-\overline{h}_T\right)+\sum_{i=1}^{M}\left[a_{Th_i}\left(Y_{i,P}-Y_{i,T}\right)\right]+$$
$$a_B\left(\overline{h}_B-\overline{h}_P\right)-\sum_{i=1}^{M}\left[a_{Bh_i}\left(Y_{i,B}-Y_{i,P}\right)\right]+\left(S^+\Delta z\right)_P-\left(S^-\Delta z\right)_P \tag{157}$$

Define:

$$a_P=a_P^\circ+a_T+a_B+\frac{\left(S^-\Delta z\right)_P+\sum_{i=1}^{M}\left[a_{Th_i}Y_{i,T}+a_{Bh_i}Y_{i,B}\right]}{\overline{h}_P} \tag{158a}$$

$$b=a_P^\circ\overline{h}_P^\circ+\left(S^+\Delta z\right)_P+\sum_{i=1}^{M}\left[\left(a_{Th_i}+a_{Bh_i}\right)Y_{i,P}\right] \tag{158b}$$

The final form of the conservation equation is obtained from Equation 157 after distributing multiplication, multiplying the negative part of the source term by $\overline{h}_P/\overline{h}_P$ to ensure that all coefficients remain positive, combining like terms, and substituting Equation 158:

$$a_P\overline{h}_P = a_T\overline{h}_T + a_B\overline{h}_B + b \tag{159}$$

At the end of a time step or iteration, the mass–weighted enthalpy ($\overline{h} = \Sigma Y_i h_i$) is known but the temperature is not known. To extract the temperature from the enthalpy, the following equation must be solved for *T*:

$$\sum_{i=1}^{M} Y_i h_i(T) = \overline{h} \tag{160}$$

where Y_i and $\overline{h}$ are known. From Equation 10, the sensible enthalpy of species *i* is:

$$\begin{aligned} h_i(T) &= \int_{T_d}^{T} \left(c_{b,i}(\theta) + c_{m,i}(\theta)\right) \mathrm{d}\theta \\ &= \frac{c_{0,i}}{n_{c,i}+1}\left(T\left(\frac{T}{T_r}\right)^{n_{c,i}} - T_d\left(\frac{T_d}{T_r}\right)^{n_{c,i}}\right) + \frac{\Delta H_{m,i}}{2}\left(\mathrm{erf}\left(\frac{T-T_{m,i}}{\sqrt{2\sigma_{m,i}^2}}\right) - \mathrm{erf}\left(\frac{T_d-T_{m,i}}{\sqrt{2\sigma_{m,i}^2}}\right)\right) \\ &= \frac{c_{0,i}T^{n_{c_i}+1}}{T_r^{n_{c_i}}\left(n_{c,i}+1\right)} - \frac{c_{0,i}T_d^{n_{c_i}+1}}{T_r^{n_{c_i}}\left(n_{c,i}+1\right)} + \frac{\Delta H_{m,i}}{2}\left(\mathrm{erf}\left(\frac{T-T_{m,i}}{\sqrt{2\sigma_{m,i}^2}}\right) - \mathrm{erf}\left(\frac{T_d-T_{m,i}}{\sqrt{2\sigma_{m,i}^2}}\right)\right) \end{aligned} \tag{161}$$

Equation 161 can also be written as:

$$h_i(T) = A_i T^{B_i} - C_i + D_i \mathrm{erf}\left(\frac{T-E_i}{F_i}\right) - G_i \tag{162a}$$

$$A_i = \frac{c_{0,i}}{\left(n_{c,i}+1\right)T_r^{n_{c,i}}} \tag{162b}$$

$$B_i = n_{c,i} + 1 \tag{162c}$$

$$C_i = \frac{c_{0,i}}{\left(n_{c,i}+1\right)}\frac{T_d^{n_{c,i}+1}}{T_r^{n_{c,i}}} \tag{162d}$$

$$D_i = \frac{\Delta H_{m,i}}{2} \tag{162e}$$

$$E_i = T_{m,i} \tag{162f}$$

$$F_i = \sqrt{2\sigma_{m,i}^2} \tag{162g}$$

$$G_i = \frac{\Delta H_{m,i}}{2}\text{erf}\left(\frac{T_d - T_{m,i}}{\sqrt{2\sigma_{m,i}^2}}\right) \tag{162h}$$

Thus, the following equation must be solved for the unknown temperature T:

$$\sum_{i=1}^{M} Y_i\left(A_i T^{B_i} - C_i + D_i\text{erf}\left(\frac{T - E_i}{F_i}\right) - G_i\right) = \bar{h} \tag{163}$$

or putting the unknown temperature on the LHS and the known terms on the RHS:

$$\sum_{i=1}^{M}\left(Y_i A_i T^{B_i} + Y_i D_i\text{erf}\left(\frac{T - E_i}{F_i}\right)\right) = \bar{h} + \sum_{i=1}^{M} Y_i\left(C_i + G_i\right) \tag{164}$$

For the special case of no melting, Equation 164 becomes:

$$\sum_{i=1}^{M} Y_i A_i T^{B_i} = \bar{h} + \sum_{i=1}^{M} Y_i C_i \tag{165}$$

Equation 164 or Equation 165 is solved for the unknown temperature T via the Newton-Raphson method.

For the special case of all species having constant (temperature invariant) specific heat capacities (i.e. $n_{c,i} = 0 \ \forall\, i$) and no melting, Equation 163 can be simplified by substituting in Equations 162b and 162d, leading to the following simple equation that can be used to extract temperature from enthalpy:

$$T - T_d = \frac{\bar{h}}{\sum_{i=1}^{M} Y_i c_{0,i}} \tag{166}$$

The reduction in CPU time offered by using Equation 166 is substantial because Newton iteration is computationally expensive.

6.9 Gas phase energy conservation

The final form of the gas phase energy equation that is solved by Gpyro is obtained by multiplying the gas phase mass conservation equation (Equation 58) by $(h_g)_P$ and subtracting the result from the gas phase energy equation (Equation 70):

$$\left(\rho_g \overline{\psi} \Delta z\right)_P^\circ \frac{h_{g,P} - h_{g,P}^\circ}{\Delta t} + \dot{m}'' h_g\Big|_b - \dot{m}'' h_g\Big|_t - h_{g,P}\dot{m}''\Big|_b + h_{g,P}\dot{m}''\Big|_t =$$
$$\overline{\psi}\rho_g D \frac{\partial h_g}{\partial z}\bigg|_b - \overline{\psi}\rho_g D \frac{\partial h_g}{\partial z}\bigg|_t + \left(\dot{Q}'''_{s-g}\Delta z\right)_P + \left(\sum_{\ell=1}^{L} \dot{Q}'''_{g,\ell}\Delta z\right)_P + \tag{167a}$$
$$\sum_{k=1}^{K}\left(\left(\dot{\omega}'''_{s,fj,k} h^*_{g,j} - \dot{\omega}'''_{s,dj,k} h_{g,j}\right)\Delta z\right)_P - \left(\dot{\omega}'''_{fg} h_g \Delta z\right)_P$$

By default, Gpyro assumes that gases produced by condensed-phase pyrolysis are generated at the gas temperature, which amounts to replacing $h^*_{g,j}$ with $h_{g,j}$ in Equation 167a. This approximation permits the simplification $\sum_{k=1}^{K}\left(\left(\dot{\omega}'''_{s,fj,k} h^*_{g,j} - \dot{\omega}'''_{s,dj,k} h_{g,j}\right)\Delta z\right)_P - \left(\dot{\omega}'''_{fg} h_g \Delta z\right)_P = 0$ because $\sum_{k=1}^{K}\left(\dot{\omega}'''_{s,fj,k} - \dot{\omega}'''_{s,dj,k}\right) = \dot{\omega}'''_{fg}$. Under these approximations, Equation 167a reduces to:

$$\left(\rho_g \overline{\psi} \Delta z\right)_P^\circ \frac{h_{g,P} - h_{g,P}^\circ}{\Delta t} + \dot{m}'' h_g\Big|_b - \dot{m}'' h_g\Big|_t - h_{g,P}\dot{m}''\Big|_b + h_{g,P}\dot{m}''\Big|_t =$$
$$\overline{\psi}\rho_g D \frac{\partial h_g}{\partial z}\bigg|_b - \overline{\psi}\rho_g D \frac{\partial h_g}{\partial z}\bigg|_t + \left(\dot{Q}'''_{s-g}\Delta z\right)_P + \left(\sum_{\ell=1}^{L} \dot{Q}'''_{g,\ell}\Delta z\right)_P \tag{167b}$$

However, the user can specify `GASES_PRODUCED_AT_TSOLID = .TRUE.` in the `&GPYRO_GENERAL` namelist group to recover the more general Equation 167a.

Equation 167b can be written as:

$$\left(\rho_g \overline{\psi} \Delta z\right)_P^\circ \frac{h_{g,P} - h_{g,P}^\circ}{\Delta t} + \dot{m}'' h_g\Big|_b - \dot{m}'' h_g\Big|_t - h_{g,P}\dot{m}''\Big|_b + h_{g,P}\dot{m}''\Big|_t =$$
$$\overline{\psi}\rho_g D \frac{\partial h_g}{\partial z}\bigg|_b - \overline{\psi}\rho_g D \frac{\partial h_g}{\partial z}\bigg|_t + \left(S\Delta z\right)_P \tag{168a}$$

$$\left(S\right)_P = \left(\dot{Q}'''_{s-g}\right)_P + \left(\sum_{\ell=1}^{L} \dot{Q}'''_{g,\ell}\Delta z\right)_P \tag{168b}$$

Now split the source term into positive and negative parts:

$$\left(S\right)_P = \left(S^+\right)_P - \left(S^-\right)_P \tag{169a}$$

In the two-temperature formulation, S^+ and S^- are calculated as:

$$\left(S^{+}\right)_P = h_{cv}T + \left(\sum_{\ell=1}^{L}\dot{Q}'''_{g,\ell}\Delta z\right)_P \tag{169b}$$

$$\left(S^{-}\right)_P = h_{cv}T_g \tag{169c}$$

It has been assumed in writing Equations 169b and 169c that $\dot{Q}'''_{g,\ell}$ is positive, i.e. there are no endothermic homogeneous gas phase reactions.

In the thermal equilibrium formulation, the gas-phase energy equation is not explicitly solved so it is not necessary to calculate S^{+} and S^{-}.

As with the gaseous species conservation equation, discretization and numerical solution of Equation 168 follows Patankar [8]. Begin by defining the following:

$$J_b = \dot{m}''h_g\Big|_b - \overline{\psi}\rho_g D\frac{\partial h_g}{\partial z}\Big|_b \tag{170a}$$

$$J_t = \dot{m}''h_g\Big|_t - \overline{\psi}\rho_g D\frac{\partial h_g}{\partial z}\Big|_t \tag{170b}$$

$$a_P^{\circ} = \frac{\left(\rho_g\overline{\psi}\Delta z\right)_P^{\circ}}{\Delta t} \tag{170c}$$

Substituting Equation 169 and Equation 170 into Equation 168 gives:

$$a_P^{\circ}\left(h_g - h_g^{\circ}\right)_P + J_b - J_t - F_b\left(h_g\right)_P + F_t\left(h_g\right)_P = \left(S^{+}\Delta z\right)_P - \left(S^{-}\Delta z\right)_P \tag{171}$$

Following Patankar [8] Equation 5.54–5.55:

$$J_b - h_{g,P}F_b = a_B\left(h_{g,P} - h_{g,B}\right) \tag{172a}$$

$$J_t - h_{g,P}F_t = a_T\left(h_{g,T} - h_{g,P}\right) \tag{172b}$$

Substituting Equation 172 into Equation 171, and multiplying the negative part of the source term by $h_{g,P}/h_{g,P}$ gives:

$$\left(a_P^{\circ} + a_B + a_T + \frac{\left(S^{-}\Delta z\right)_P}{h_{g,P}}\right)h_{g,P} = a_P^{\circ}h_{g,P}^{\circ} + a_B h_{g,B} + a_T h_{g,T} + \left(S^{+}\Delta z\right)_P \tag{173}$$

Define:

$$b = a_P^{\circ} h_{g,P}^{\circ} + \left(S^{+}\Delta z\right)_P \tag{174a}$$

$$a_P = a_P^{\circ} + a_B + a_T + \frac{\left(S^{-}\Delta z\right)_P}{h_{g,P}} \tag{174b}$$

After substituting Equation 174 into Equation 173, the final form of the discretized equation becomes:

$$a_P h_{g,P} = a_B h_{g,B} + a_T h_{g,T} + b \tag{175}$$

The coefficients a_B and a_T are obtained from Equation 127 by substituting $\Gamma = \rho_g \psi D$.

6.10 Gas phase momentum conservation

Begin with Equation 75:

$$\frac{\left(\frac{P\overline{M}}{RT_g}\overline{\psi}\Delta z\right)_P - \left(\frac{P\overline{M}}{RT_g}\overline{\psi}\Delta z\right)_P^{\circ}}{\Delta t} = \left(\frac{\overline{K}}{\nu}\right)_b \left.\frac{\partial P}{\partial z}\right|_b - \left(\frac{\overline{K}}{\nu}\right)_t \left.\frac{\partial P}{\partial z}\right|_t + \left(\dot{\omega}_{fg}'''\Delta z\right)_P$$
$$-\left(\left(\frac{\overline{K}}{\nu}\rho_g g\right)_b - \left(\frac{\overline{K}}{\nu}\rho_g g\right)_t\right)$$

Replace the pressure gradient with its discrete approximation:

$$-\left(\frac{\overline{K}}{\nu}\right)_b \left.\frac{\partial P}{\partial z}\right|_b \approx -\left(\frac{\overline{K}}{\nu}\right)_b \frac{P_B - P_P}{\left(\delta z\right)_b} \tag{176a}$$

$$-\left(\frac{\overline{K}}{\nu}\right)_t \left.\frac{\partial P}{\partial z}\right|_t \approx -\left(\frac{\overline{K}}{\nu}\right)_t \frac{P_P - P_T}{\left(\delta z\right)_t} \tag{176b}$$

Expand the first term on the LHS as:

$$\frac{\left(\frac{P\overline{M}}{RT_g}\overline{\psi}\Delta z\right)_P - \left(\frac{P\overline{M}}{RT_g}\overline{\psi}\Delta z\right)_P^{\circ}}{\Delta t} \equiv \left(\frac{\overline{M}\overline{\psi}\Delta z}{RT_g\Delta t}\right)_P^{\circ}\left(P_P - P_P^{\circ}\right) + P_P\left(\left(\frac{\overline{M}\overline{\psi}\Delta z}{RT_g\Delta t}\right)_P - \left(\frac{\overline{M}\overline{\psi}\Delta z}{RT_g\Delta t}\right)_P^{\circ}\right) \tag{177}$$

Substituting Equations 176 and 177 into Equation 75 gives:

$$\left(\frac{\overline{M}\overline{\psi}\Delta z}{RT_g\Delta t}\right)_P^{\circ}\left(P_P-P_P^{\circ}\right)+P_P\left(\left(\frac{\overline{M}\overline{\psi}\Delta z}{RT_g\Delta t}\right)_P-\left(\frac{\overline{M}\overline{\psi}\Delta z}{RT_g\Delta t}\right)_P^{\circ}\right)-\left(\frac{\overline{K}}{\nu}\right)_b\frac{P_B-P_P}{(\delta z)_b}+$$
$$\left(\frac{\overline{K}}{\nu}\right)_t\frac{P_P-P_T}{(\delta z)_t}=\left(\dot{\omega}_{fg}'''\Delta z\right)_P-\left(\left(\frac{\overline{K}}{\nu}\rho_g g\right)_b-\left(\frac{\overline{K}}{\nu}\rho_g g\right)_t\right) \tag{178}$$

Define:

$$a_P^{\circ}=\left(\frac{\overline{M}\overline{\psi}\Delta z}{RT_g\Delta t}\right)_P^{\circ} \tag{179a}$$

$$a_T=\frac{\left(\overline{K}/\nu\right)_t}{(\delta z)_t} \tag{179b}$$

$$a_B=\frac{\left(\overline{K}/\nu\right)_b}{(\delta z)_b} \tag{179c}$$

Substitute Equation 179 into Equation 178:

$$a_P^{\circ}\left(P_P-P_P^{\circ}\right)-a_B\left(P_B-P_P\right)+a_T\left(P_P-P_T\right)=$$
$$-P_P\left(\left(\frac{\overline{M}\overline{\psi}\Delta z}{RT_g\Delta t}\right)_P-a_P^{\circ}\right)+\left(\dot{\omega}_{fg}'''\Delta z\right)_P-\left(\left(\frac{\overline{K}}{\nu}\rho_g g\right)_b-\left(\frac{\overline{K}}{\nu}\rho_g g\right)_t\right) \tag{180}$$

Distribute multiplication and combine like terms:

$$\left(a_P^{\circ}+a_B+a_T\right)P_P=a_P^{\circ}P_P^{\circ}+a_BP_B+a_TP_T-P_P\left(\left(\frac{\overline{M}\overline{\psi}\Delta z}{RT_g\Delta t}\right)_P-a_P^{\circ}\right)+$$
$$\left(\dot{\omega}_{fg}'''\Delta z\right)_P-\left(\left(\frac{\overline{K}}{\nu}\rho_g g\right)_b-\left(\frac{\overline{K}}{\nu}\rho_g g\right)_t\right) \tag{181}$$

Define:

$$a_P=a_P^{\circ}+a_B+a_T \tag{182a}$$

$$b=a_P^{\circ}P_P^{\circ}-P_P\left(\left(\frac{\overline{M}\overline{\psi}\Delta z}{RT_g\Delta t}\right)_P-a_P^{\circ}\right)+\left(\dot{\omega}_{fg}'''\Delta z\right)_P-\left(\left(\frac{\overline{K}}{\nu}\rho_g g\right)_b-\left(\frac{\overline{K}}{\nu}\rho_g g\right)_t\right) \tag{182b}$$

Substituting Equation 182 into Equation 181 gives:

$$a_P P_P = a_B P_B + a_T P_T + b \tag{183}$$

6.11 Extension to two dimensions

The equations presented above are given in one dimensional form. Extension to two dimensions is straightforward. As an example, the condensed-phase energy conservation equation is extended to two dimensions in this section. This section should be compared to Section 6.8.

The two-dimensional analog to Equation 151 is:

$$\begin{aligned}\left(\overline{\rho}\Delta z\Delta x\right)_P^\circ \frac{\overline{h}_P - \overline{h}_P^\circ}{\Delta t} &= -\dot{q}''\Big|_b \Delta x + \dot{q}''\Big|_t \Delta x - \dot{q}''\Big|_e \Delta z + \dot{q}''\Big|_w \Delta z - \left(\dot{Q}'''_{s-g}\Delta z\Delta x\right)_P \\ &+ \left(\sum_{k=1}^{K} \dot{Q}'''_{s,k}\Delta z\Delta x\right)_P - \left(\frac{\partial \dot{q}''_r}{\partial z}\Delta z\Delta x\right)_P + \sum_{i=1}^{M}\left(\left(\dot{\omega}'''_{fi} - \dot{\omega}'''_{di}\right)h_i \Delta z\Delta x\right)_P + \overline{h}_P\left(\dot{\omega}'''_{fg}\Delta z\Delta x\right)_P\end{aligned} \tag{184}$$

Where *e* and *w* denote the east and west interfaces between cells.

Equation 184 can be written as:

$$\left(\overline{\rho}\Delta z\Delta x\right)_P^\circ \frac{\overline{h}_P - \overline{h}_P^\circ}{\Delta t} = -\dot{q}''\Big|_b \Delta x + \dot{q}''\Big|_t \Delta x - \dot{q}''\Big|_e \Delta z + \dot{q}''\Big|_w \Delta z + \left(S\Delta z\Delta x\right)_P \tag{185a}$$

$$\left(S\right)_P = \left(\sum_{k=1}^{K} \dot{Q}'''_{s,k}\Delta z\right)_P - \left(\frac{\partial \dot{q}''_r}{\partial z}\right)_P + \sum_{i=1}^{M}\left(\left(\dot{\omega}'''_{fi} - \dot{\omega}'''_{di}\right)h_i\right)_P + \overline{h}_P\left(\dot{\omega}'''_{fg}\right)_P - \dot{Q}'''_{s-g} \tag{185b}$$

Where $\dot{Q}'''_{s-g}$ is calculated per Equation 63. For numerical convenience, the source term (Equation 185b) is split into its positive and negative components:

$$S_P = \left(S^+\right)_P - \left(S^-\right)_P \tag{186a}$$

$$\left(S^+\right)_P = h_{cv}T_{g,P} - \left(\frac{\partial \dot{q}''_r}{\partial z}\right)_P + \sum_{i=1}^{M}\left(\dot{\omega}'''_{fi}h_i\right)_P + \overline{h}_P\left(\dot{\omega}'''_{fg}\right)_P + \sum_{k=1}^{K}\max\left(\dot{Q}'''_{s,k},0\right) + \max\left(\dot{Q}'''_{s-g},0\right) \tag{186b}$$

$$\left(S^-\right)_P = h_{cv}T_P + \sum_{i=1}^{M}\left(\dot{\omega}'''_{di}h_i\right)_P - \sum_{k=1}^{K}\min\left(\dot{Q}'''_{s,k},0\right) - \min\left(\dot{Q}'''_{s-g},0\right) \tag{186c}$$

To facilitate use of the efficient Thomas algorithm/TDMA solver to solve Equation 185, the heat conduction terms must be expressed in terms of enthalpy, i.e.:

$$\begin{aligned}\dot{q}''\big|_t &= -\bar{k}_t \frac{\partial T}{\partial z}\bigg|_t \equiv -\left(\frac{\bar{k}}{\bar{c}}\right)_t \left(\frac{\partial \bar{h}}{\partial z}\bigg|_t - \sum_{i=1}^{M}\left(h_i \frac{\partial Y_i}{\partial z}\right)_t\right) \\ &\approx -\left(\frac{\bar{k}}{\bar{c}}\right)_t \frac{\bar{h}_P - \bar{h}_T}{(\delta z)_t} + \sum_{i=1}^{M}\left[\left(\frac{\bar{k}}{\bar{c}} h_i\right)_t \frac{Y_{i,P} - Y_{i,T}}{(\delta z)_t}\right]\end{aligned} \tag{187a}$$

$$\begin{aligned}\dot{q}''\big|_b &= -\bar{k}_b \frac{\partial T}{\partial z}\bigg|_b \equiv -\left(\frac{\bar{k}}{\bar{c}}\right)_b \left(\frac{\partial \bar{h}}{\partial z}\bigg|_b - \sum_{i=1}^{M}\left(h_i \frac{\partial Y_i}{\partial z}\right)_b\right) \\ &\approx -\left(\frac{\bar{k}}{\bar{c}}\right)_b \frac{\bar{h}_B - \bar{h}_P}{(\delta z)_b} + \sum_{i=1}^{M}\left[\left(\frac{\bar{k}}{\bar{c}} h_i\right)_b \frac{Y_{i,B} - Y_{i,P}}{(\delta z)_b}\right]\end{aligned} \tag{187b}$$

$$\begin{aligned}\dot{q}''\big|_w &= -\bar{k}_w \frac{\partial T}{\partial x}\bigg|_w \equiv -\left(\frac{\bar{k}}{\bar{c}}\right)_w \left(\frac{\partial \bar{h}}{\partial x}\bigg|_w - \sum_{i=1}^{M}\left(h_i \frac{\partial Y_i}{\partial x}\right)_w\right) \\ &\approx -\left(\frac{\bar{k}}{\bar{c}}\right)_w \frac{\bar{h}_P - \bar{h}_W}{(\delta x)_w} + \sum_{i=1}^{M}\left[\left(\frac{\bar{k}}{\bar{c}} h_i\right)_w \frac{Y_{i,P} - Y_{i,W}}{(\delta x)_w}\right]\end{aligned} \tag{187c}$$

$$\begin{aligned}\dot{q}''\big|_e &= -\bar{k}_e \frac{\partial T}{\partial x}\bigg|_e \equiv -\left(\frac{\bar{k}}{\bar{c}}\right)_e \left(\frac{\partial \bar{h}}{\partial x}\bigg|_e - \sum_{i=1}^{M}\left(h_i \frac{\partial Y_i}{\partial x}\right)_e\right) \\ &\approx -\left(\frac{\bar{k}}{\bar{c}}\right)_e \frac{\bar{h}_E - \bar{h}_P}{(\delta x)_e} + \sum_{i=1}^{M}\left[\left(\frac{\bar{k}}{\bar{c}} h_i\right)_e \frac{Y_{i,E} - Y_{i,P}}{(\delta x)_e}\right]\end{aligned} \tag{187d}$$

Substituting Equations 186 and 187 into Equation 185 gives:

$$\begin{aligned}\frac{(\bar{\rho}\Delta z \Delta x)_P^{\circ}}{\Delta t}\left(\bar{h}_P - \bar{h}_P^{\circ}\right) = &-\left(\frac{\bar{k}}{\bar{c}}\right)_t \frac{\bar{h}_P - \bar{h}_T}{(\delta z)_t}\Delta x + \sum_{i=1}^{M}\left[\left(\frac{\bar{k}}{\bar{c}} h_i\right)_t \frac{Y_{i,P} - Y_{i,T}}{(\delta z)_t}\right]\Delta x \\ &+\left(\frac{\bar{k}}{\bar{c}}\right)_b \frac{\bar{h}_B - \bar{h}_P}{(\delta z)_b}\Delta x - \sum_{i=1}^{M}\left[\left(\frac{\bar{k}}{\bar{c}} h_i\right)_b \frac{Y_{i,B} - Y_{i,P}}{(\delta z)_b}\right]\Delta x \\ &-\left(\frac{\bar{k}}{\bar{c}}\right)_w \frac{\bar{h}_P - \bar{h}_W}{(\delta x)_w}\Delta z + \sum_{i=1}^{M}\left[\left(\frac{\bar{k}}{\bar{c}} h_i\right)_w \frac{Y_{i,P} - Y_{i,W}}{(\delta x)_w}\right]\Delta z \\ &+\left(\frac{\bar{k}}{\bar{c}}\right)_e \frac{\bar{h}_E - \bar{h}_P}{(\delta x)_e}\Delta z - \sum_{i=1}^{M}\left[\left(\frac{\bar{k}}{\bar{c}} h_i\right)_e \frac{Y_{i,E} - Y_{i,P}}{(\delta x)_e}\right]\Delta z \\ &+\left(S^{+}\Delta z \Delta x\right)_P - \left(S^{-}\Delta z \Delta x\right)_P\end{aligned} \tag{188}$$

Define:

$$a_P^{\circ} = \frac{(\bar{\rho}\Delta z \Delta x)_P^{\circ}}{\Delta t} \tag{189a}$$

$$a_T = \frac{\left(\bar{k}/\bar{c}\right)_t}{\left(\delta z\right)_t}\Delta x \tag{189b}$$

$$a_B = \frac{\left(\bar{k}/\bar{c}\right)_b}{\left(\delta z\right)_b}\Delta x \tag{189c}$$

$$a_W = \frac{\left(\bar{k}/\bar{c}\right)_w}{\left(\delta x\right)_w}\Delta z \tag{189d}$$

$$a_E = \frac{\left(\bar{k}/\bar{c}\right)_e}{\left(\delta x\right)_e}\Delta z \tag{189e}$$

$$a_{Th_i} = \frac{\left(\bar{k}h_i/\bar{c}\right)_t}{\left(\delta z\right)_t}\Delta x \tag{189f}$$

$$a_{Bh_i} = \frac{\left(\bar{k}h_i/\bar{c}\right)_b}{\left(\delta z\right)_b}\Delta x \tag{189g}$$

$$a_{Wh_i} = \frac{\left(\bar{k}h_i/\bar{c}\right)_w}{\left(\delta x\right)_w}\Delta z \tag{189h}$$

$$a_{Eh_i} = \frac{\left(\bar{k}h_i/\bar{c}\right)_e}{\left(\delta x\right)_e}\Delta z \tag{189i}$$

The coefficients in the numerator of Equations 189b –189i are calculated using harmonic means (see Equation 128). Substitute Equation 189 into Equation 188:

$$\begin{aligned} a_P^\circ\left(\bar{h}_P - \bar{h}_P^\circ\right) = \quad & -a_T\left(\bar{h}_P - \bar{h}_T\right) + \sum_{i=1}^{M}\left[a_{Th_i}\left(Y_{i,P} - Y_{i,T}\right)\right] \\ & + a_B\left(\bar{h}_B - \bar{h}_P\right) - \sum_{i=1}^{M}\left[a_{Bh_i}\left(Y_{i,B} - Y_{i,P}\right)\right] \\ & - a_W\left(\bar{h}_P - \bar{h}_W\right) + \sum_{i=1}^{M}\left[a_{Wh_i}\left(Y_{i,P} - Y_{i,W}\right)\right] \\ & + a_E\left(\bar{h}_E - \bar{h}_P\right) - \sum_{i=1}^{M}\left[a_{Eh_i}\left(Y_{i,E} - Y_{i,P}\right)\right] \\ & + \left(S^+\Delta z\Delta x\right)_P - \left(S^-\Delta z\Delta x\right)_P \end{aligned} \tag{190}$$

Define:

$$a_P = a_P^\circ + a_T + a_B + a_E + a_W + \frac{\left(S^- \Delta z\right)_P + \sum_{i=1}^{M}\left[a_{Th_i} Y_{i,T} + a_{Bh_i} Y_{i,B} + a_{Wh_i} Y_{i,W} + a_{Eh_i} Y_{i,E}\right]}{\overline{h}_P} \quad (191a)$$

$$b = a_P^\circ \overline{h}_P^\circ + \left(S^+ \Delta z \Delta x\right)_P + \sum_{i=1}^{M}\left[\left(a_{Th_i} + a_{Bh_i} + a_{Wh_i} + a_{Eh_i}\right) Y_{i,P}\right] \quad (191b)$$

The final form of the conservation equation is obtained from Equation 190 after distributing multiplication, multiplying the negative part of the source term by $\overline{h}_P / \overline{h}_P$ to ensure that all coefficients remain positive, combining like terms, and substituting Equation 191:

$$a_P \overline{h}_P = a_T \overline{h}_T + a_B \overline{h}_B + a_W \overline{h}_W + a_E \overline{h}_E + b \quad (192)$$

The two dimensional governing equations are solved with a line-by-line TDMA where alternating "sweeps" are made in the *x* and *z* directions. In a *z*-direction sweep, the $a_W \overline{h}_W$ and $a_E \overline{h}_E$ terms are treated as source terms, i.e. the discretization equations are:

$$a_P \overline{h}_P = a_T \overline{h}_T + a_B \overline{h}_B + b_z \quad (193a)$$

$$b_z = b + a_W \overline{h}_W + a_E \overline{h}_E \quad (193b)$$

Equation 193a is then solved with the method described in Section 6.2.

In an *x*-direction sweep, the $a_T \overline{h}_T$ and $a_B \overline{h}_B$ terms are treated as source terms, i.e. the discretization equations are:

$$a_P \overline{h}_P = a_W \overline{h}_W + a_E \overline{h}_E + b_x \quad (194a)$$

$$b_x = b + a_T \overline{h}_T + a_B \overline{h}_B \quad (194b)$$

Equation 194a is then solved with the method described in Section 6.2.

7.0 MATERIAL PROPERTY ESTIMATION

To apply Gpyro to real–world combustible solids, the model input parameters required to characterize these materials must be established. Unfortunately, we have a limited ability to extract the required material properties from laboratory experiments such as the Cone Calorimeter, Fire Propagation Apparatus, thermogravimetric analysis, and differential scanning calorimetry. This is the biggest barrier preventing increased application of research–type pyrolysis models for practical purposes.

7.1 Background

Although techniques have been developed to estimate several material fire properties from laboratory fire tests, there is a disconnect between the material properties needed for numerical pyrolysis modeling and those properties that can be determined with existing techniques. This chapter presents a methodology that uses an automated optimization method based on a genetic algorithm (GA) to extract the material properties needed for numerical pyrolysis modeling from laboratory experiments, particularly traditional bench–scale flammability tests (cone calorimeter, FPA) and small–scale thermal analysis (TGA). This chapter is based on a paper published in *Fire Safety Journal* [10].

Genetic algorithms are a class of search tools that use the principles of Darwinian evolution to seek an optimal solution to a problem. In contrast to many classical search methods, genetic algorithms can handle nonlinear problems and search spaces having high dimensionality, i.e. a large number of adjustable parameters. The proposed methodology involves simulating a laboratory test or tests with the generalized pyrolysis model described earlier, and using a genetic algorithm to locate a set of model parameters (or "material properties") that provide optimal agreement between the model calculations and the experimental data, subject to the constraints imposed by the model and the experiments.

Optimization techniques based on genetic algorithms are "embarrassingly parallel", meaning that they can be easily divided into a large number of parallel tasks that can run on a separate CPU or core. The actual computer implementation of the genetic algorithm optimization methodology presented here has been parallelized using Message Passing Interface. The parallel code has been successfully run on Linux computer clusters at UC Berkeley using more than 60 CPUs. The code is massively parallel, meaning that it can use as many CPUs or cores as are available in a networked computer cluster.

The material properties found by the genetic algorithm will be close to the "actual" values provided: 1) the experimental measurements are sufficiently accurate and contain enough information to establish a unique set of model parameters, 2) the pyrolysis model is an adequate representation of the underlying physical processes, and 3) the specified boundary and initial conditions are an accurate representation of the experimental configuration. This approach is self–consistent in the sense that the same model that is used to estimate the material properties from small–scale experimental data can be coupled to a CFD code to model large–scale fire development.

The pyrolysis model described earlier can be used to simulate both traditional flammability tests (cone calorimeter, FPA) as well as TGA experiments. When samples are instrumented with thermocouples, cone calorimeter and FPA experiments can provide information regarding a material's thermal properties, but probably cannot be used to establish detailed kinetics mechanisms. In comparison, TGA provides no information about a material's thermal properties, but provides detailed information about a material's decomposition kinetics. Differential scanning calorimetry or differential thermal analysis could potentially be used to infer specific heat capacity and heats of reaction. Due to the different types of information that can be obtained from flammability tests and thermal analysis experiments, both are potentially useful for material property estimation for pyrolysis modeling.

7.2 Genetic algorithm for estimating material properties

In this section, a methodology is presented that can be used to estimate unknown model input parameters from experimental data. It involves using a genetic algorithm to find a set of model input parameters that provides near–optimal agreement between the calculations of the generalized pyrolysis model and experimental measurements from a laboratory test. However, this inverse problem is ill–posed. That is, the solution (the set of model input parameters) is not necessarily unique and it is not necessarily stable to small changes in the input data. The proposed methodology is heuristic, meaning that the final solution is not necessarily the absolute optimal solution; however, the algorithm will find a solution that gives a near–optimal prediction of the experimental data given the constraints of the underlying physical model. That is, the results are almost as good as those that would be obtained with the optimal solution.

Genetic and evolutionary algorithms have been previously used in engineering. They have already been applied to the optimization of combustion and chemical kinetics problems, including heterogeneous [11] and homogeneous [12] reaction mechanisms. However, since the use of a GA to estimate solid phase material properties from fire test data is a specialized application, the algorithm used here is described in detail below. It is presented within the context of using cone calorimeter or FPA–type experiments for property estimation, but the basic methodology also applies to thermal analysis experiments (TGA, DSC, DTA). The reader desiring a general treatment of genetic or evolutionary algorithms is referred to several books covering the topic [13–15].

7.2.1 Initial population

The search process is initialized by randomly generating several candidate solutions (for the idealized charring material described earlier, this would be a vector of eight real numbers corresponding to k_v, c_v, Z, E, ΔH_{vol}, k_c, ρ_c, and c_c). Each candidate solution is referred to as an *individual* or a *chromosome*, and the terms are used interchangeably throughout the genetic algorithms literature. A single parameter of an individual (or chromosome) is referred to as a *gene*, for example the numerical value of the virgin phase thermal conductivity is one gene. The entire group of candidate solutions is referred to as a *population*. Typical population sizes range from tens to hundreds of individuals. Populations constantly evolve to form subsequent *generations*; the initial population is the first generation, the offspring of the first generation make up the second generation, and so on.

This chapter adopts a separate nomenclature from the rest of the dissertation. Let $\{a_1, a_2 \ldots a_n\}$ denote the n parameters, or genes, that make up an individual, or chromosome. Here, a_1 may be associated with k_v, a_2 with c_v, and so on. For certain variables that may take on values over several orders of magnitude, it is convenient to have the gene represent the logarithm of that variable. Let $\{A^1, A^2 \ldots A^N\}$ denote the N individuals that make up the population. The nomenclature $A^I(\ell)$ is used to denote the I^{th} individual of generation ℓ. Similarly, $A_j^I(\ell)$ represents the j^{th} gene of the I^{th} individual of generation ℓ.

Begin by generating an initial population:

$$A_j^I(1) = a_{j,\min} + r_j^I\left(a_{j,\max} - a_{j,\min}\right) \tag{195}$$

The parameters $a_{j,max}$ and $a_{j,min}$ are the user–specified upper and lower bounds of each variable; all parameters are constrained by these values throughout the evolution process. In Equation 195, r_j^I is an N by n matrix of random real numbers distributed uniformly on the interval [0, 1]. The indices I and j are cycled from 1 to N and 1 to n, respectively.

7.2.2 Fitness

Next, the *fitness* of each individual is evaluated. Here, fitness is a measure of how well the candidate solution matches the experimental data. For demonstration purposes, it is assumed in the following discussion that the experimental data is obtained from a flammability test such as the cone calorimeter. It is also assumed that at a minimum, surface temperature and mass loss rate histories are available. Extension to additional measurements (e.g., in–depth thermocouple temperature measurements) or experimental configurations (e.g., TGA) is straightforward. The residuals that measure the level of agreement between the measured surface temperature/mass loss rate histories and the predictions of individual I are:

$$E_{T_s}^I = \frac{1}{n_{\Delta t}} \sum \left(\frac{T_{s,exp}}{\left| T_{s,try}^I - T_{s,exp} \right| + \varepsilon_{T_s} T_{s,exp}} \right)^{\zeta} \tag{196a}$$

$$E_{\dot{m}''}^I = \frac{1}{n_{\Delta t}} \sum \left(\frac{\dot{m}''_{exp}}{\left| \dot{m}''^I_{try} - \dot{m}''_{exp} \right| + \varepsilon_{\dot{m}''} \dot{m}''_{exp}} \right)^{\zeta} \tag{196b}$$

Here, a subscript "exp" denotes the experimental data, and a subscript "try" denotes the trial solution generated by a certain set of parameters contained in the individual. The parameter ε is a user–specified small number that prevents the fitness from approaching infinity as the first term in the denominator approaches zero, and ζ is a user–specified exponent. Equation 196 is written as a summation, rather than an integral, because experimental measurements are obtained at discrete time intervals. In Equation 196a, the summation is performed for surface temperature measurements/predictions only before the experimentally determined ignition time, but in

Equation 196b the summation for the mass loss rate measurements/predictions is carried out over the entire duration of the test. This choice was made because the accuracy of surface temperature measurement becomes more questionable after ignition.

Next, the weighted fitness of individual *I* is calculated as:

$$\widetilde{f}^{I} = \phi_{T_s} E^{I}_{T_s} + \phi_{\dot{m}''} E^{I}_{\dot{m}''} \tag{197}$$

the ϕ factors are user–specified constants that determine the relative importance of each fitness metric. If experimental data are obtained at multiple heat flux levels (or heating rates in the case of TGA experiments), then an individual's final fitness is considered to be the sum of the fitness values calculated at each heat flux level:

$$f^{I} = \sum_{n_{\dot{q}''_e}} \widetilde{f}^{I} \tag{198}$$

where $n_{\dot{q}''_e}$ is the number of heat flux levels (or heating rates) at which data were obtained. The steps represented by Equations 196 through 198 are then repeated for all individuals to tabulate a numerical fitness value for each individual.

7.2.3 Selection for reproduction

The next generation is obtained through the reproduction process wherein parents' genes are combined to produce offspring. The likelihood that an individual reproduces is determined by its fitness. In this way, relatively bad candidate solutions die out, while relatively good solutions survive and propagate. This "natural selection" process is the basis of genetic algorithms' ability to exploit good solutions.

There are many different ways in which individuals can be selected for reproduction, but proportional selection [15] is used here for simplicity. The selection probability of individual *I* is:

$$p^{I}_{sel} = \frac{f^{I}}{\sum_{I=1}^{N} f^{I}} \tag{199}$$

Thus, the higher an individual's fitness, the greater the probability it will be selected for reproduction. In practice, the selection probability in Equation 199 is implemented by first sorting the current population in order of decreasing fitness, i.e. $f^{I} \geq f^{I+1}$. Then, for each individual, the following is calculated:

$$q^{I} = \sum_{i=I}^{N} p^{i}_{sel} \tag{200}$$

Note that by definition, $q^1 = 1$ and $q^N = p_{sel}^N$. Next, a random number r belonging to a uniform distribution is generated on the interval [0, 1]. Selection proceeds by comparing r with q: if $q^{I+1} < r \le q^I$, then A^I is selected for reproduction. The selection process is repeated N times to choose N parents.

If one individual has a relative fitness much higher than the average fitness, it is likely that this individual will be selected several times for reproduction. To prevent premature convergence, a target (maximum) selection number S is used so that any individual may be selected for reproduction no more than S times per generation ($1 \le S < N$). If an individual has reproduced S times and is selected again for reproduction, then a new individual is randomly selected from the population for reproduction. Low values of S preserve variability at the expense of convergence.

7.2.4 Reproduction

Once individuals have been selected for reproduction, offspring are generated through a linear combination of two parents. Denote $\{B\}$ as the subset of population $\{A\}$ that was selected for reproduction. As many as S copies of a single individual may belong to the set $\{B\}$. The offspring are stored in a temporary intermediate population denoted $\{C\}$. This is accomplished by generating a matrix of random numbers (denoted r_j^i where $i = 1 \ldots N/2$ and $j = 1 \ldots n$) belonging to a uniform distribution on the interval [–0.5, 0.5] and then producing offspring as linear combinations of the parents:

$$\begin{aligned} C_j^I &= r_j^i B_j^I + \left(1 - r_j^i\right) B_j^{I+1} \\ C_j^{I+1} &= r_j^i B_j^{I+1} + \left(1 - r_j^i\right) B_j^I \end{aligned} \qquad \text{for } I = 1, 3, 5 \ldots N-1 \quad \text{where} \quad i = \frac{I+1}{2} \tag{201}$$

7.2.5 Mutation

After two parents have combined genes to produce a new individual, a process analogous to genetic mutation is used to introduce variability into the population, which ensures the entire search space is explored and that the solution does not become trapped at a local maximum. Mutation is accomplished by introducing random variations into one or more of an individual's genes. The probability that a gene is mutated is relatively low, perhaps 0.05. Mutation is performed on a gene–by–gene basis. At the start of the calculation, each parameter (gene) is assigned a user–specified mutation probability $p_{mut,j}$. Mutation is performed on the intermediate population $\{C\}$ and begins by generating a matrix of random numbers, denoted r_j^I (where $I = 1 \ldots N$ and $j = 1 \ldots n$) belonging to a uniform distribution on the interval [0,1]. Mutation occurs on individual I gene j if $r_j^I \le p_{mut,j}$. If a gene is selected for mutation, then one of two types of equiprobable mutation occur. In the first (Equation 202a) the gene is simply replaced with a randomly generated value. In the second, the gene is replaced with an excursion from its current value (Equation 202b):

$$C_j^I = a_{j,\min} + r\left(a_{j,\max} - a_{j,\min}\right) \tag{202a}$$

$$C_{\mathrm{j}}^{I} = C_{\mathrm{j}}^{I} + s\, v_{mut}\left(a_{j,\max} - a_{j,\min}\right) \tag{202b}$$

In Equation 202a, r is a random number on the interval [0, 1], and in Equation 202b s is a random number on the interval [–0.5, 0.5]. The user–specified parameter v_{mut} controls the severity of the mutation and is generally less than 1.

7.2.6 Replacement

The final step in the genetic algorithm is to replace the parents with the offspring. In the algorithm used here, the offspring (i.e., the individuals in the intermediate population) completely replace the parents:

$$A^{I}\left(\ell+1\right) = C^{I}\left(\ell\right) \quad \text{for } I = 1,2,3,\ \ldots\ N \tag{203}$$

The processes of selection, reproduction, and mutation and replacement are repeated until a predetermined number of generations has passed or the solution converges, meaning no further improvement of the solution occurs with subsequent generations.

7.3 Application to a synthetic material with known properties

To assess the methodology's capabilities, a hypothetical charring material with a thickness of 10 mm is used to generate a set of simulated experimental data under nonflaming conditions at 25 kW/m^2 and 75 kW/m^2 irradiance. A known set of input parameters is used to generate synthetic experimental data, i.e. real experimental data are not used. This represents a situation where the thermophysical properties of an idealized material are known exactly, and provides an opportunity to see how closely the genetic algorithm can match these known properties.

The overall fitness is evaluated from the surface temperature, back face temperature, mass loss rate, and cumulative mass loss. All eight ϕ values are set to 1, a value of $\varepsilon = 0.1$ is used, and the fitness exponent ζ is set to 2. In this case, the maximum attainable fitness is $8/\varepsilon^{\zeta} = 800$.

The evolution of the population–averaged fitness and the fitness of the best individual found at any point during the evolution process are shown in Figure 2. The average fitness, an indication of the quality of the "gene pool", increases rapidly for the first ~40 generations but increases only slightly or plateaus thereafter. By 150 generations, the highest fitness found during in the evolution process reached over 600, or 75% of the maximum attainable fitness (800). For practical situations, it would have been adequate to stop the algorithm after ~150 generations.

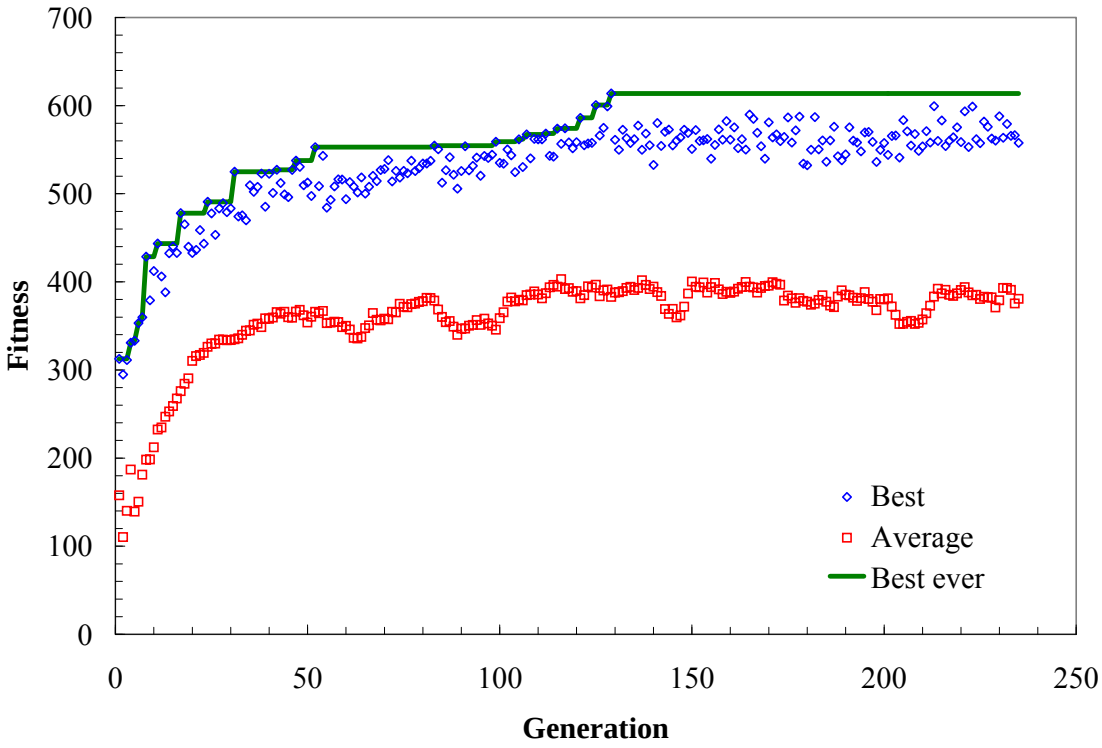

Figure 2. Evolution of average and best fitness to ~250 generations for simulated experimental data case.

Table 3 gives a comparison of the optimal values found by the genetic algorithm and the actual values used to generate the simulated experimental data. The algorithm matched 7 of 13 parameters within 10%. The biggest error was for the specific heat capacity temperature exponents. The lower value of the pre–exponential factor found by the genetic algorithm is compensated for by the slightly lower activation energy. This compensation effect between the pre–exponential factor and the activation energy has long been observed to occur in the estimation of pyrolysis kinetics parameters from thermogravimetric analysis. Due to the kinetic compensation effect, the algorithm may not find the "true" values of the pre–exponential factor and the activation energy, but it will find values of these parameters that match the Arrhenius function over the temperature range within which pyrolysis occurs.

Table 3. Comparison of actual material properties used to generate simulated experimental data and material properties found with genetic algorithm.

Property	Actual	GA	% Error
Pre–exponential factor (s^{-1})	2.00×10^{11}	1.56×10^{10}	–92.2
Activation energy (kJ/mol)	142.0	130.4	–8.2
Reaction order (–)	2.00	1.90	–5.0
Char density (kg/m^3)	100.0	102.9	2.9
Heat of pyrolysis (J/kg)	5.00×10^5	5.21×10^5	4.1
Virgin conductivity @ 300 K (W/m–K)	0.200	0.207	3.6
Char conductivity @ 300 K (W–m–K)	0.060	0.095	59.0
Virgin conductivity temperature exponent (–)	0.500	0.397	–20.5
Char conductivity temperature exponent (–)	0.800	0.395	–50.6
Virgin specific heat @ 300 K (J/kg–K)	1400	1333	–4.8
Char specific heat @ 300 K (J/kg–K)	1600	1610	0.6
Virgin specific heat temperature exponent (–)	0.200	0.379	89.6
Char specific heat temperature exponent (–)	0.100	0.477	376.8

A comparison of the simulated experimental surface temperature, back face temperature, and mass loss rate with the model predictions using the optimal material properties found by the genetic algorithm is given in Figure 3. It is seen that the agreement is excellent, which verifies the methodology's capabilities to estimate material properties from experimental data.

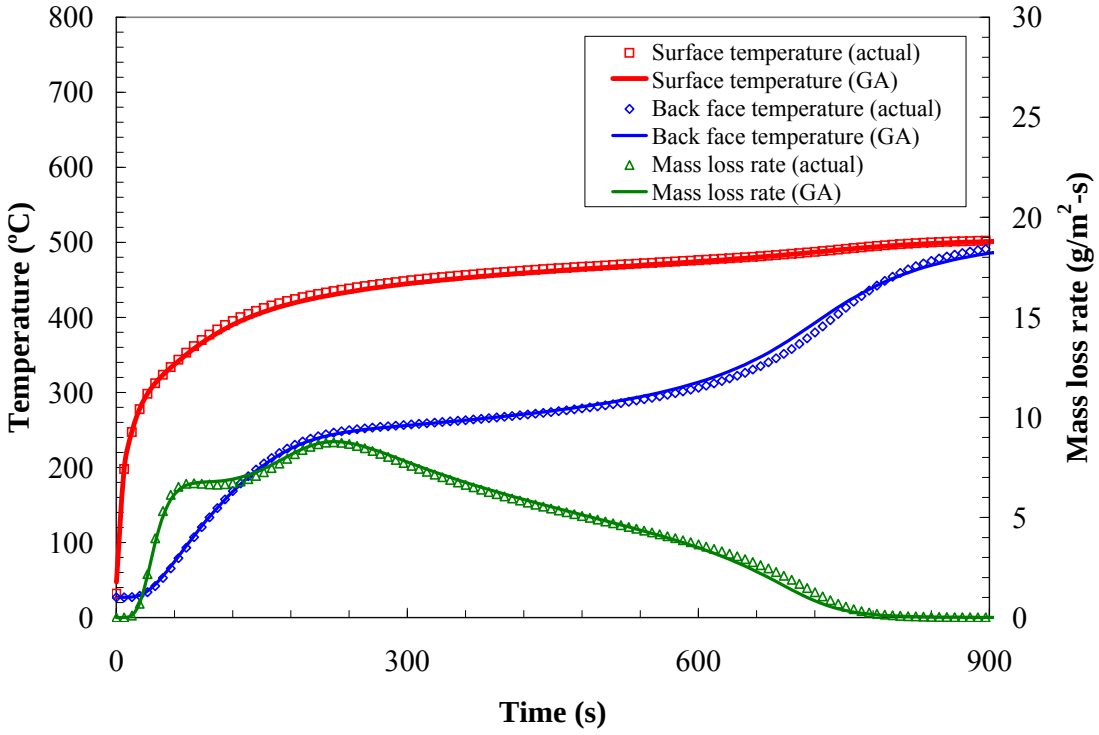

(a)

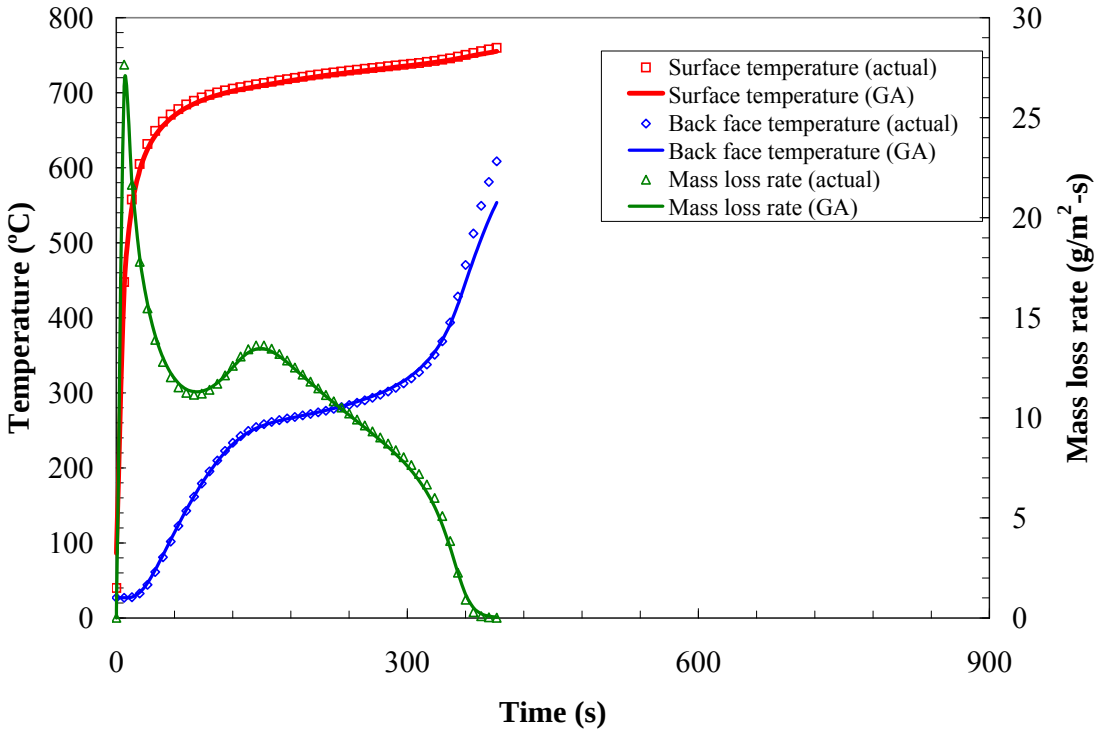

(b)

Figure 3. Comparison of simulated experimental data and model calculations using optimized material properties determined by GA.
(a) 25 kW/m^2 irradiance; (b) 75 kW/m^2 irradiance.

8.0 CONCLUDING REMARKS

This technical reference presents the mathematical formulation of Gpyro. The document is constantly updated, so if parts of it are not clear, please let us know. Similarly, if there are features or functionality you would like to see added, please let us know, and they may make it into the next release of Gpyro!

9.0 REFERENCES

[1] Lautenberger, C., "Gpyro – A Generalized Pyrolysis Model for Combustible Solids – Users' Guide," Version 0.800, May 1, 2014.

[2] Lautenberger, C.W., "A Generalized Pyrolysis Model for Combustible Solids," Ph.D. Dissertation, Department of Mechanical Engineering, University of California, Berkeley, Fall 2007. http://reaxengineering.com/media/docs/lautenberger_dissertation.pdf

[3] Lautenberger, C. & Fernandez-Pello, A.C., "Generalized Pyrolysis Model for Combustible Solids," *Fire Safety Journal* **44** 819-839 (2009)..

[4] Lautenberger, C. & Fernandez-Pello, A.C., "A Model for the Oxidative Pyrolysis of Wood," *Combustion and Flame* **156** 1503-1513 (2009).

[5] Dodd, A.B., Lautenberger, C. & Fernandez-Pello, A.C., "Numerical Examination of Two-Dimensional Smolder Structure in Polyurethane Foam," *Proceedings of the Combustion Institute* **32**: 2497-2504 (2009).

[6] Lautenberger, C., Kim, E., Dembsey, N. & Fernandez-Pello, C., "The Role of Decomposition Kinetics in Pyrolysis Modeling – Application to a Fire Retardant Polyester Composite," *Fire Safety Science* **9**: 1201-1212 (2008).

[7] Bird, R.B., Stewart, W.E., and Lightfoot, E.N., *Transport Phenomena*, John Wiley & Sons, New York, 1960.

[8] Patankar, S.V., *Numerical Heat Transfer and Fluid Flow*, Hemisphere Publishing Corporation, New York, 1980.

[9] Mills, A.F., *Mass Transfer*, Prentice Hall, Upper Saddle River, NJ, 2001, pg. 161.

[10] Lautenberger, C., Rein, G., and Fernandez–Pello, C., "The application of a genetic algorithm to estimate material properties for fire modeling from bench–scale fire test data," *Fire Safety Journal* **41**: 204–214 (2006).

[11] Park, T.Y. and Froment, G.F., "A hybrid genetic algorithm for the estimation of parameters in detailed kinetic models," *Computers & Chemical Engineering* **22**: S103–S110 (1998).

[12] Elliott, L., Ingham, D.B., Kyne, A.G., Mera, N.S., Pourkashanian M., and Wilson, C.W., "Genetic algorithms for optimisation of chemical kinetics reaction mechanisms," *Progress in Energy and Combustion Science* **30**: 297–328 (2004).

[13] Goldberg, D., *Genetic Algorithms: In Search, Optimization & Machine Learning*. Addison–Wesley Publishing Company, Inc., Menlo Park, 1989.

[14] Michalewicz, Z., *Genetic Algorithms + Data Structures = Evolution Programs*. Springer–Verlag, New York, 1992.

[15] Dumitrescu D., Lazzerini B., Jain, L.C., and Dumitrescu A., *Evolutionary Computation*. CRC Press, New York, 2000.